Available online at www.sciencedirect.com
ScienceDirect
Ore Geology Reviews xx (2007) xxx–xxx
ORE GEOLOGY REVIEWS
www.elsevier.com/locate/oregeorev

Sanjiang Tethyan metallogenesis in S.W. China: Tectonic setting, metallogenic epochs and deposit types

Zengqian Hou [a,*], Khin Zaw [b], Guitang Pan [c], Xuanxue Mo [d], Qiang Xu [c], Yunzhong Hu [a], Xingzhen Li [c]

[a] *Institute of Geology, Chinese Academy of Geological Sciences, Beijing 100037, PR China*
[b] *Centre for Ore Deposit Research, University of Tasmania, Private Bag 79, Hobart, Tasmania, 7001, Australia*
[c] *Chengdu Institute of Geology and Mineral Resources, Chengdu, PR China*
[d] *China University of Geosciences, Beijing 100082, PR China*

Received 23 December 2002; accepted 24 December 2004

Abstract

Tectonically, the Sanjiang Tethyan Metallogenic Domain (STMD) is located within the eastern Himalayan–Tibetan Orogen in the Sanjiang Tethys, southwestern China. Although this metallogenic domain was initiated in the Early Palaeozoic, extensive metallogenesis occurred in the Late Palaeozoic, Late Triassic and Himalayan (Tertiary) epochs. Corresponding tectonic settings and environments in the domain are: an arc-basin system related to the subduction of the Palaeo-Tethyan oceanic slabs; a post-collision crustal extension setting caused by the lithospheric delamination or slab breakoff underneath the Sanjiang Tethys during the Late Triassic; large-scale strike-slip faulting and thrusting systems due to the Indo-Asian continent collision since the Palaeocene. In this metallogenic domain important gold, copper, base metals, rare metals and tin ore belts, incorporating a large number of giant deposits, were developed. The main types of deposits include: (1) porphyry copper deposits, controlled by a large-scale strike-slip fault system, (2) VHMS deposits, mainly occurring in intra-arc rift basins and post-collision crustal extensional basins, (3) shear-zone type gold deposits in the ophiolitic mélange zone along the thrusting–shearing system, (4) hydrothermal silver-polymetallic deposits in the Triassic intra-continental rift basins and Tertiary strike-slip pull-apart basins, and (5) Himalayan granite-related greisen-type tin and rare-metallic deposits. Within the metallogenic epochs of the Late Palaeozoic to Cenozoic, the styles and types of the ore deposits changed from VHMS types in the Late Palaeozoic through exhalative-sedimentary type deposits in the Late Triassic, to porphyry-type copper deposits, shear-zone type gold deposits, hydrothermal vein-type silver-polymetallic deposits, greisen-type tin and rare-metal deposits in the Cenozoic. Correspondingly, ore-forming metals also changed from a Pb–Zn–Cu–Ag association through Ag–Cu–Pb–Zn, Fe–Ag–Pb and Ag–Au–Hg associations, to Ag–Cu–Pb–Zn, Cu–Mo, Au, Sn, and Li–Rb–Cs–Nb–Zr–Hf–Y–Ce–Sc associations.

Keywords: Sanjiang Tethyan metallogenesis; Tectonic setting; Metallogenic epochs; Deposit types; S.W. China

1. Introduction

The Sanjiang Tethyan Metallogenic Domain (STMD) in southwestern China forms a significant part of the Tethyan metallogenic belt, one of three giant

* Corresponding author.
E-mail address: hzq@cags.net.cn (Z. Hou).

0169-1368/$ - see front matter © 2007 Published by Elsevier B.V.
doi:10.1016/j.oregeorev.2004.12.007

Table 1
Geological features of major ore deposits in the Sanjiang Tethyan Metallogenic Domain (STMD)

Name	County, province	Long./ lat.	Metallic comm.	Tonnage	Grade	Tectonic setting and environment	Host rock	Alteration	Ore minerals	Size	Shape	Genetic type	Data source
Yulong (1)	Jamda, Tibet	97°44′ 31°24′	Cu–Mo	Cu: 6.5 Mt	Cu: 0.99% Mo:0.028%	Large-scale strike-slip fault belt, Changdu–Simao block	Monzonitic granite porphyry, quartz monzonitic porphyry, Triassic sandstone and mudstone	Outwards from center: potassic alteration →quartz sericite zone →argillization →propylitization	Chalcopyrite, molybdenite, pyrite, bornite, tetrahedrite, cubanite, sphalerite, galena, native gold, native silver	Bedded orebody: thickness: 72 m prime orebody: diameter: 1000 m depth: 500 m	Irregular prism	Porphyry Cu–Mo deposit	Tang and Luo (1995), Hou et al. (2003a)
Mangzong (2)	Jamda, Tibet	97°45′ 31°20′	Cu–Mo	Cu: 0.25 Mt	Cu: 0.34% Mo: 0.03%	Large-scale strike-slip fault belt, Changdu–Simao block	Monzonitic granite porphyry	Outwards from center: potassic alteration →quartz sericite zone →propylitization	Chalcopyrite, pyrite, molybdenite, galena, sphalerite, tennantite, chalcocite	Prime orebody: diameter: 400 m depth: 400 m	Irregular pipe	Porphyry Cu–Mo deposit	Tang and Luo (1995), Hou et al. (2003a)
Zhanaga (3)	Jamda, Tibet	97°43′ 31°20′	Cu–Mo	Cu: 0.3 Mt	Cu: 0.36% Mo: 0.03%	Large-scale strike-slip fault belt, Changdu–Simao block	Monzonitic granite porphyry; syenitic granite porphyry	From south to north: tourmalinization (quartz sericite zone) →argillization →propylitization	Chalcopyrite, molybdenite, pyrite, magnetite, chalcocite, bismuthinite	Prime orebody diameter: 350 m depth: 540 m	Prism	Porphyry Cu–Mo deposit	Tang and Luo (1995), Hou et al. (2003a)
Duoxiasongduo (4)	Jamda, Tibet	97°55′ 31°10′	Cu–Mo	Cu: 0.5 Mt	Cu: 0.38% Mo:0.04%	Large-scale strike-slip fault belt, Changdu–Simao block	Alkali-feldspar granite porphyry; Monzonitic granite porphyry	Outwards from center: potassic alteration →quartz sericite zone →propylitization	Chalcopyrite, pyrite, molybdenite, magnetite, galena, sphalerite, bornite	Prime orebody: diameter: 500 m depth: 570 m	Irregular prism	Porphyry Cu–Mo deposit	Tang and Luo (1995), Hou et al. (2003a)
Malasongduo (5)	Jamda, Tibet	98°00 ′ 31°00′	Cu–Mo	Cu: 1.0 Mt	Cu: 0.44% Mo: 0.14%	Large-scale strike-slip fault belt, Changdu–Simao block	Monzonitic granite porphyry; syenitic granite porphyry	Outwards from center: potassic alteration →quartz sericite zone →argillization →propylitization	Chalcopyrite, pyrite molybdenite, galena, sphalerite, bornite, tetrahedrite	Prime orebody: diameter: 960 m depth: 694 m	Irregular prism	Porphyry Cu–Mo deposit	Tang and Luo (1995), Hou et al. (2003a)
Mamupu (6)	Mangkang, Tibet	98°30 ′ 30°00′	Cu–Au	No data	Cu: 0.12–0.32% Au: 6.4–13.1 g/t	Large-scale strike-slip fault belt, Changdu–Simao block	Syenitic porphyry	No zoning	Chalcopyrite, pyrite, molybdenite, galena, sphalerite, native gold	No data	Irregular	Porphyry Cu–Au deposit	Tang and Luo (1995)

Zhaokalong (7)	Yushu, Qinghai	97°21′ 32°38′	Fe–Pb–Zn–Ag	Fe: 11 Mt	Total Fe: 31.8–47.1% Pb: 0.001–4.12% Zn: 0.05–1.02% Ag: 6.5–191.5 g/t	Post-collision crustal extension environment, Jinshajiang orogenic belt	Siltstone, slate, dolomite, limestone and andesite	Baritization, sericitization, chloritization	Siderite, magnetite, galena, sphalerite, chalcopyrite, pyrite, bornite	Orebody: length: 18–428 m width: 2–50 m	Layered, stratabound, lenticular	VHMS deposit	Liu et al. (1993)
Jiaduoling (8)	Jamda, Tibet	98°05 ′ 31°50′	Fe	No data	No data	Post-collision crustal extension environment, Jinshajiang orogenic belt	Triassic dioritic porphyry	Albitization, sericitization, chloritization	No data	No data	Layered, stratabound, lenticular	Porphyry Fe deposit ?	Hou et al. (2003b)
Luchun (9)	Deqin, Yunnan	98°42′ 28°05′	Cu–Zn–Pb	Cu:0.3 Mt Pb+Zn: 0.4 Mt	Cu: 0.65% Pb: 0.76–1.67% Zn: 0.98–4.49%	Post-collision crustal extension environment Jinshajiang orogenic belt	Bimodal suite: felsic volcanic rock	Silicification, sericitization, chloritization	Chalcopyrite, pyrite, galena, magnetite, pyrrhotite, sphalerite	Orebody: length: 20–1000 m width: 10–50 m	Layered, stockwork	VHMS deposit	Wang et al. (2002)
Yargla (10)	Deqin, Yunnan	99°10′ 29°20′	Cu–Zn	Cu: 1 Mt Pb+Zn: 3 Mt	Cu: 0.6%	Intra-oceanic arc, Jinshajiang orogenic belt	Calc-alkaline andesitic–dacitic volcanic rocks	Chloritization, skarnization	Chalcopyrite, pyrite, magnetite, galena, sphalerite	Orebody length: 1500–1700 m	Stratabound, lenticular	VHMS deposit	Zhan et al. (1998)
Gala (11)	Garze, Sichuan	99°15′ 31°50′	Au	Au: >20 t	Au: 3.3–8.0 g/t	Garze shear belt, Garze–Litang suture zone	Ophiolitic suite: Triassic basaltic rocks	Silicification, sericitization, carbonatization, pyritization	Pyrite, arsenopyrite, stibnite, native gold	8 orebodies Length: 300–700 m Width: 100–150 m Thickness: 0.9–32 m	Stratabound, lenticular	Shear-zone deposit	Zhang et al. (1998a)
Erze (12)	Muli, Sichuan	110°28′ 28°18′	Au–Ag–Cu	Au: 10.8 t	Au: 4.7–7.8 g/t Ag: 10–50 g/t Cu: 0.5–2.5%	Continental basement of Triassic Yidun arc	Upper Permian marble, dolomitic limestone, phyllite and mica schist	Sericitization, pyritization, carbonatization	Pyrite, chalcopyrite, arsenopyrite, tetrahedrite, siderite	3 main orebodies: length: 110–420 m width: 5–90 m thickness: 34–78 m	Sheet, vein, lenticular, irregular	Vein-type deposit	Liu et al. (1993)
Gayiqiong (13)	Baiyu, Sichuan	99°18′ 31°34′	Zn–Pb–Cu–Ag	Zn+Pb+Cu: 0.5 Mt	Pb: 3.12% Zn: 3.49%	Intra-arc rift zone, Triassic Yidun arc	Bimodal suite; dacitic volcaniclastic pile, and associated siderite and jasper	Potassic alteration, silicification, sericitization	Pyrite, sphalerite, galena, tetrahedrite, chalcopyrite, arsenopyrite	5 orebodies: length: 200–400 m thickness: 4–32 m	Bedded, stockwork	Kuroko-type VHMS deposit	Hou et al. (1995, 2001a)

(continued on next page)

Table 1 (*continued*)

Name	County, province	Long./ lat.	Metallic comm.	Tonnage	Grade	Tectonic setting and environment	Host rock	Alteration	Ore minerals	Size	Shape	Genetic type	Data source
Gacun (14)	Baiyu, Sichuan	99°32′ 31°11′	Zn–Pb–Cu–Ag	Zn+Pb+Cu: 4 Mt, Ag: 3800 t	Zn: 5.4% Pb: 3.7% Cu: 0.44% Ag: 160 g/t	Intra-arc rift zone, Triassic Yidun arc	Bimodal suite; rhyolitic volcaniclastic pile and associated jasper, barite, and dolomite	Silicification, sericitization, chloritization, epidotization	Pyrite, sphalerite, galena, tetrahedrite, chalcopyrite, arsenopyrite, bornite	Mineralized zone: length: 950–1870 m width: 200–1870 m thickness: 0.5–51.62 m	Sheet-like, stockwork	Kuroko-type VHMS deposit	Hou et al. (1995, 2001a)
Kongmasi (15)	Baiyu, Sichuan	99°10′ 31°30′	Hg	Hg: 1879 t	Hg: 0.1%	Inner-volcanic arc, Triassic Yidun arc	High-K rhyolitic volcanic rocks and limestone	Silicification, sericitization, carbonatization, pyritization	Metacinnabar, pyrite, sphalerite, galena, orpiment, psilomelane, pyrolusite, rhodochrosite	Orebody: length: 858 m thickness: 0.7–6.4 m	Semi-layered	Vein-type deposit	Hou et al. (1995)
Nongduke (16)	Baiyu, Sichuan	99°24′ 30°56′	Ag–Au	Ag: 1300 t Au: 1.3 t	Ag: 20 0 g/t Au: 2–10 g/t	Miange back-arc basin, Triassic Yidun arc	Late Triassic high-K rhyolitic rocks	Silicification, sericitization, pyritization	Stibnite, tennanite, pyrite, sphalerite, orpiment, realgar, native gold	Orebody: length: 120–300 m width: 30–50 m	Bedded, vein-like	Epithermal vein-type deposit	Qu et al. (2001)
Xuejiping (17)	Zhongdian, Yunnan	99°50′ 28°02′	Cu	Cu: 0.30 Mt	Cu: 0.60%	Zhongdian arc (south), Triassic Yidun arc	Dioritic porphyry and monozonitic porphyry	Silicification, chloritization, actinolization	Chalcopyrite, pyrite, magnetite	6 orebodies: length: 200–650 m thickness: 20–80 m	Veinlet-disseminated	Porphyry Cu deposit	Hou et al. (2001a)
Hongshan (18)	Zhongdian, Yunnan	99°53′ 28°07′	Cu–Pb–Zn–Ag	Cu: 0.29 Mt	Cu: 1.1%	Zhongdian arc (south), Triassic Yidun arc	Layered skarn between Triassic slate and felsic intrusion	Skarnization	Chalcopyrite, pyrite, magnetite, galena, sphalerite	20 orebodies: length: 30–1223 m thickness: 3.9–19.6 m	Layered, massive	Skarn-type deposit	Hou et al. (2001a)
Cuomolong (19)	Batang, Sichuan	99°22′ 30°30′	Sn–Pb–Zn	Sn: 11,511 t	Sn: 0.22–1.38% Pb: 0.3–0.5% Zn: 0.5–2.5%	Margin of the Zongza continental block	Skarn between granite and Triassic sandstone	Skarnization	Pyrite, magnetite, cassiterite, galena, sphalerite	15 orebodies: length: 84–442 m thickness: 1.4–8.5 m	Lenticular, stratabound	Skarn–type ? deposit	Ye et al. (1992)

Xiasai (20)	Batang, Sichuan	99°36′ 30°27′	Ag–Pb–Zn	Ag: 5600 t	Ag: 300 g/t Pb: 8% Zn: 2%	Triassic Yidun arc	Upper Triassic sandstone and slate sequence	Silicification, sericitization	Galena, sphalerite, pyrite, native silver	5 orebodies: length: 1000–2200 m width: 5–80 m	Vein	Vein-type deposit	Hou et al. (1995)
Najiaoxi (21)	Batang, Sichuan	99°21′ 29°22′	Pb–Zn	Pb: 0.24 Mt Zn: 0.26 Mt	Zn: 36% Pb: 3.4%	Margin of the Zongza continental block	Cambrian crystalline limestone and dolomite	Silicification, sericitization, carbonization	Pyrite, sphalerite, magnetite, galena	Orebody: length: 320 m width: 25 m	Stratabound, lenticular	Skarn-type deposit	Ye et al. (1992)
Baiyangping (22)	Lanping, Yunnan	99°15′ 26°52′	Cu–Co–Ag	In exploring	Cu: 0.93–2.9% Co: 0.10–0.27%	Strike-slip pull-apart basin, Lanping large-scale basin	Cretaceous transitional zone between porous sandstone and low-permeability carbonaceous bargillite	Silicification, carbonization, chloritization, epidotization	Tetrahedrite, pyrite, chalcopyrite, galena, freibergite	4 orebodies: length: 510–810 m thickness: 1.6–4.3 m	Large veins or lenses	Vein-type polymetallic deposit	Wang et al. (2000a,b)
Fulongchang (23)	Lanping, Yunnan	99°14′ 26°49′	Cu–Ag–Pb	In exploring	Cu: 1.4–9.5% Ag: 51–502 g/t Pb: 4.2%	Strike-slip pull-apart basin, Lanping large-scale basin	Cretaceous transitional zone between porous sandstone and low-permeability carbonaceous argillite	Silicification, carbonization	Tetrahedrite, pyrite, chalcopyrite, galena, freibergite	4 orebodies: length: 750–1500 m thickness: 1.2–2.5 m	Large veins or lenses	Vein-type polymetallic deposit	Wang et al. (2000a,b)
Yanzidong (24)	Lanping, Yunnan	99°18′ 26°45′	Pb–Zn–Cu–Ag	In exploring	No data	Late Triassic rifting basin, Lanping large-scale basin	Upper Triassic dolomitic limestone, limestone breccia, sandstone and conglomerate	Carbonization, chloritization, baritization, celesitization	Bornite, tennantite, tetrahedrite, pyrite, chalcopyrite, galena, siderite, freibergite	No data	Stratabound, sheet-like	Sedex deposit	Wang et al. (2000a,b)
Huishan (25)	Lanping, Yunnan	99°17′ 26°43′	Pb–Zn–Cu–Ag	In exploring	No data	Late Triassic rifting basin, Lanping large-scale basin	Upper Triassic siliceous rocks, dolomitic limestone and limestone breccia	Carbonization, chloritization, baritization, celesitization	Galena, sphalerite, pyrite, chalcopyrite, bornite	No data	Stratabound, lenticular	Sedex deposit	Wang et al. (2000a,b)
Jinding (26)	Lanping, Yunnan	99°25′ 26°24′	Zn–Pb–Ag	Zn: 12.84 Mt Pb: 2.64 Mt	Zn: 8.32–10.52% Pb: 1.16–2.42% Ag: 12.5–12.6 g/t	Strike-slip pull-apart basin, Lanping large-scale basin	Tertiary argillaceous dolomite, argillaceous siltstone, sandstone and siltstone	Pyritization, marcasitization, calcitization, dolomitization, hematization, silicification, baritization,	Galena, sphalerite, pyrite, pyrrhotite, marcasite, chalcopyrite, native silver	Orebody: length: 50–1450 m thickness: 10–102 m depth: 2 1 5 –	Stratabound, lenticular	Sedex deposit	Liu et al. (1993)

(continued on next page)

Table 1 (*continued*)

Name	County, province	Long./ lat.	Metallic comm.	Tonnage	Grade	Tectonic setting and environment	Host rock	Alteration	Ore minerals	Size	Shape	Genetic type	Data source
Baiyangchang (27)	Yunlong, Yunnan	99°24′ 26°07′	Ag–Cu–Pb–Zn	Exploring	Ag: 110–245 g/t Cu: 0.36–1.61% Pb: 0.22–3.24% Zn: 1.11%	Strike-slip pull-apart basin, Lanping large-scale basin	Jurassic–Cretaceous high-porous limestone and the overlying low-porous carbargillite	celesitization Baritization, carbonatization, decolouration	Tennantite, chalcopyrite, bornite, freibergite, pyrite, argentite, sphalerite, galena, native silver	1360 m Orebody: length: 150–405 m thickness: 2.7–17.7 m	Large vein, stratabound, banded	Sedex deposit	Ye et al. (1992)
Diantan (28)	Tengchong, Yunnan	98°26′ 25°39′	Sn	No data	No data	Chayu–Tengchong granitoid belt, eastern segment of Gangdese magmatic arc	Mesozoic biotite granite, dolomitic limestone, arenaceous mudstone and sandstone	Skarnization, silicification, sericitization, chloritization	Pyrite, cassiterite, galena, sphalerite, magnetite, pyrrhotite	No data	Lens, stratabound	Skarn-type Sn deposit	Liu et al. (1993)
Datongchang (29)	Tengchong, Yunnan	98°44′ 25°32′	Sn	Sn: <10,000 t	Sn: 0.016–0.26% Pb: 0.67–15.7% Zn: 1–35% Cu: 0.38–1.08% Ag: 1–326.8 g/t	Chayu–Tengchong granitoid belt, Eastern segment of Gangdese magmatic arc	Mesozoic biotite granite, dolomitic limestone, arenaceous mudstone and sandstone	Skarnization, silicification, tremolitization, sericitization, chloritization, fluoritization	Pyrite, cassiterite, galena, sphalerite, magnetite, pyrrhotite	Orebody: length: 10–100 m thickness: 1–12 m depth: 20–200 m	Vein, stratabound	Sn-bearing Sulphide type deposit	Ye et al. (1992)
Xiaolonghe (30)	Tengchong, Yunnan	98°26′ 25°27′	Sn	Sn: 26,200 t	Sn: 0.18–0.42%	Chayu–Tengchong granitoid belt; eastern segment of Gangdese magmatic arc	Mesozoic biotite granite, sandy slate	Greisenization, sericitization, silicification, chloritization	Pyrite, topaz, cassiterite, magnetite	Orebody: length: 30–300 m thickness: 1–20 m	Irregular	Cassiterite–sulphide type deposit	Liu et al. (1993)
Gudong (31)	Tengchong, Yunnan	98°30′ 25°20′	Sn	No data	No data	Chayu–Tengchong granitoid belt; eastern segment of Gangdese magmatic arc	Mesozoic biotite granite, sandy slate	Greisenization, sericitization, silicification, chloritization	Pyrite, topaz, cassiterite, magnetite	No data	No data	Cassiterite–sulphide type deposit	Liu et al. (1993)

Tieyaoshan (32)	Tengchong, Yunnan	98°24′ 25°15′	Sn	No data	No data	Chayu–Tengchong granitoid belt; eastern segment of the Gangdese magmatic arc	Mesozoic biotite granite, sandy slate	Greisenization, sericitization, silicification, chloritization	Pyrite, topaz, cassiterite, magnetite	No data	No data	Cassiterite–sulphide type deposit	Liu et al. (1993)
Laopingshan (33)	Tengchong, Yunnan	98°22′ 25°00′	Sn	No data	No data	Chayu–Tengchong granitoid belt; eastern segment of Gangdese magmatic arc	Mesozoic biotite granite, sandy slate	Greisenization, sericitization, silicification, chloritization	Pyrite, topaz, cassiterite, magnetite	No data	No data	Cassiterite–sulphide type deposit	Liu et al. (1993)
Lailishan (34)	Lianghe, Yunnan	98°16′ 24°55′	Sn	Sn: 42,600 t	Sn: 0.63–1.58%	Chayu–Tengchong granitoid belt; eastern segment of Gangdese magmatic arc	Himalayan K-feldspar granite; metamorphosed feldspathic sandstone, argillaceous siltstone, dolomite	Potassic alteration kaolinization, sericitization, silicification, pyritization, chloritization	Pyrite, topaz, pyrrhotite, cassiterite	Orebody: length: 40–600 m width: 0.89–23.85 m	Vein, stratabound	Cassiterite–sulphide type deposit	Liu et al. (1993)
Shuiyinchang (35)	Baoshan Yunnan	98°57′ 25°20′	Hg	No data	No data	Baoshan continental block	Devonian–Carboniferous limestone formation	Silicification, pyritization, dolomitization	Pyrite, cinnabar, sphalerite, galena	No data	No data	Vein-type Hg deposit	Liu et al. (1993)
Maocaopo (36)	Baoshan, Yunnan	98°54′ 24°22′	Hg	No data	No data	Baoshan continental block	Devonian–Carboniferous limestone formation	Silicification, pyritization, dolomitization	Pyrite, cinnabar, sphalerite, galena	No data	No data	Vein-type Hg deposit	Liu et al. (1993)
Dongshan (37)	Baoshan, Yunnan	99°11′ 24°26′	Pb–Zn	No data	No data	Baoshan continental block	Early-Palaeozoic limestone formation	Silicification, pyritization, chloritization, dolomitization,	Pyrite, sphalerite, galena, pyrrhotite	No data	No data	Massive sulphide deposit	Liu et al. (1993)
Mengxing (38)	Baoshan, Yunnan	99°11′ 23°52′	Pb–Zn	No data	No data	Baoshan continental block	Early-Palaeozoic limestone formation	Silicification, pyritization, chloritization, dolomitization,	Pyrite, sphalerite, galena, pyrrhotite	No data	No data	Massive sulphide deposit	Liu et al. (1993)
Shihuangchang (39)	Nanjian, Yunnan	100°09′ 25°19′	Au–Sb–As	No data	No data	Late Triassic rift basin, Simao continental block	Upper Triassic limestone and sandy-slate	Silicification, sericitization, pyritization, dolomitization	Pyrite, realgar, orpiment, sphalerite, galena	No data	Vein, irregular	Vein-type Au–Sb–As deposit	Liu et al. (1993)

(continued on next page)

Table 1 (*continued*)

Name	County, province	Long./ lat.	Metallic comm.	Tonnage	Grade	Tectonic setting and environment	Host rock	Alteration	Ore minerals	Size	Shape	Genetic type	Data source
Maanshan (40)	Nanjian Yunnan	100°03′ 25°15′	Hg	Hg: <1000 t	Hg: 0.05–0.2%	Late Triassic rift basin, Simao continental block	Upper Triassic slate and limestone	Pyritization, dolomitization, silicification, calcitization	Pyrite, cinnabar , sphalerite, galena	No data	Vein, lentiform	Vein-type Hg deposit	Liu et al. (1993)
Zhacun (41)	Nanjian Yunnan	100°10′ 25°07′	Au	Au: <10 t	Au 2.16–3.55 g/t	Late Triassic rift basin, Simao continental block	Feldspathic sandstone, carbonaceous argillite, siltstone, shale	Pyritization, dolomitization, silicification, calcitization, baritization	Pyrite, ankerite, galena, sphalerite, native gold	Orebody: length: 720–800 m thickness: 3.41–5.23 m	Lentiform, stratabound	Vein-type Au deposit	Liu et al. (1993)
Bijiashan (42)	Nanjian, Yunnan	100°00′ 25°00′	Au	No data	No data	Late Triassic rift basin, Simao continental block	Feldspathic sandstone, argillite, siltstone, shale	Pyritization, dolomitization, silicification, calcitization	Pyrite, ankerite, galena, sphalerite, native gold	No data	Lentiform, stratabound	Vein-type Au deposit	Liu et al. (1993)
Tongchangjie (43)	Yunxian, Yunnan	99°45′ 24°20′	Cu	Cu: 0.2 Mt	Cu: 1.54%	Changning–Menglian palaeo-backarc basin	Permo-Carboniferous mafic volcanic sequence	Silicification, sericitization, chloritization, carbonatization	Pyrrhotite pyrite, chalcopyrite, sphalerite, galena, hematite, magnetite	Massive orebody: length: 110–600 m thickness: 1–5 m	Stratabound, lentiform	VHMS deposit	Yang and Mo (1993); Yang et al. (1992)
Laochang (44)	Lanchang, Yunnan	99°44′ 22°45′	Pb–Zn–Ag	Pb: 0.51 Mt Zn: 0.16 Mt Ag: >500 t	Pb: 1.21–8.90% Zn: 2.89–5.09% Ag: 57.5–195 g/t	Changning–Menglian palaeo-backarc basin	Trachybasaltic–andesitic lava and associated volcaniclastics; and metamorphosed basaltic volcaniclastics intercalated with jasper	Silicification, sericitization, tremolitization, epidotization, chloritization, carbonatization	Pyrrhotite, sphalerite, pyrite, galena, chalcopyrite, magnetite	Orebody: length: 10–750 m thickness: 0.1–40 m	Stratabound, lentiform	VHMS deposit	Yang and Mo (1993); Yang et al. (1992)
Denghaishan (45)	Simao, Yunnan	100°52′ 23°40′	Cu	No data	No data	Simao continental block	Jurassic–Tertiary sandstone formation	No data	Chalcocite, bornite, covellite chalcopyrite, malachite, pyrite, cuprite	No data	Stratabound, lentiform	Sandstone-type Cu deposit	Liu et al. (1993)
Bailong (46)	Simao, Yunnan	100°55′ 23°05′	Cu	No data	No data	Simao continental block	Jurassic–Tertiary sandstone formation	No data	Chalcocite, bornite, covellite, chalcopyrite, malachite, pyrite, cuprite	No data	Stratabound, lentiform	Sandstone-type Cu deposit	Liu et al. (1993)
Yaojiashan (47)	Simao, Yunnan	101°43′ 22°23′	Cu	No data	No data	Simao continental block	Jurassic–Tertiary sandstone formation	No data	Chalcocite, bornite, covellite chalcopyrite, malachite, pyrite, cuprite	No data	Stratabound, lentiform	Sandstone-type Cu deposit	Liu et al. (1993)

Laownagzhai (48)	Qingyuan, Yunnan	101°27′ 23°54′	Au	Au: 106 t	Au: 3.7–7.7 g/t	Ailaoshjan shear belt, Jinshajiang (Ailaoshan) suture zone	Palaeozoic greywacke, mafic tuff and basaltic lava	Silicification, sericitization, carbonatization, pyritization, chloritization	Pyrite, arsenopyrite, stibnite, native gold, sphalerite, chalcopyrite, tetrahedrite	Orebody: length: 80–1050 m thickness: 1.5–27.7 m	Vein, irregular, stratabound, lentiform	Shear zone-type deposit	Liu et al. (1993), Hu et al. (1995)
Donggualin (49)	Zhenyuan, Yunnan	101°26′ 23°53′	Au	Au: 50 t	Au: 5.2 g/t	Ailaoshjan shear belt, Jinshajiang (Ailaoshan) suture zone	Palaeozoic siliceous slate, meta-quartzite, sandstone, and lamprophyre	Silicification, sericitization, carbonatization, pyritization, chloritization	Pyrite, arsenopyrite, stibnite, native gold, sphalerite, chalcopyrite, tetrahedrite	Orebody: length: 520–560 m thickness: 5–65 m	Bedded, lentiform	Shear zone-type deposit	Hu et al. (1995)
Lannitang (50)	Zhenyuan, Yunnan	101°25′ 23°52′	Au	No data	Au: 5.0 g/t	Ailaoshjan shear belt, Jinshajiang (Ailaoshan) suture zone	Palaeozoic ultramafic rock, basaltic lavas, greywacke and lamprophyre	Silicification, sericitization, carbonatization, pyritization, chloritization	Pyrite, arsenopyrite, stibnite, native gold, sphalerite, chalcopyrite, tetrahedrite	Orebody: length: 180–550 m thickness: 2.6–30 m	Bedded, lentiform	Shear zone-type deposit	Hu et al. (1995)
Jinchang (51)	Mojiang, Yunnan	101°45′ 23°30′	Au	Au: 27 t	Au: 1–55.45 g/t	Ailaoshjan megashear belt, Jinshajiang (Ailaoshan) suture zone	Palaeozoic tuffaceous sandstone, siltstone, basaltic rocks, augite peridotite	Silicification, pyritization, sericitization, serpentinization, chloritization, carbonatization	Pyrite, tetrahedrite, chalcopyrite, gersdorffite, millerite	Mineralized zone: length: 3200 m width: 50–400 m thickness: 59m	Vein, irregular, lentiform	Shear zone-type deposit	Liu et al. (1993), Hu et al. (1995)
Daping (52)	Yuanyang, Yunnan	102°59′ 22°51′	Au	Au: >20 t	Au: 1–32.5 g/t	Ailaoshjan shear belt, Jinshajiang (Ailaoshan) suture	Diorite, granite porphyry, lamprophyre, siliceous shale, sandstone, limestone	Sericitization, carbonatization, chloritization, silicification, tremolitization, epidotization, pyritization	Sphalerite, pyrite, galena, chalcopyrite, tetrahedrite, pyrrhotite, chalcocite	Orebody: length: 500–1000 m thickness: 0.4–2 m depth: 100–300 m	Vein, irregular, lentiform	Shear zone-type deposit	Hu et al. (1995)
Dapingzhang (53)	Simao, Yunan	100°31′ 22°47′	Cu–Pb–Zn	Cu: 0.3 Mt Pb: 0.15 Mt Zn: 0.15 Mt	Cu: 1.93–6.1% Pb: 0.2–1.1% Zn: 0.4–1.8%	Paleozoic Zuogong–Jinghong volcanic arc	Quartz keratophyre, arc spillite–keratophyre sequence	Silicification, sericitization, chloritization	Sphalerite, pyrite, chalcopyrite, pyrrhotite	Orebody: length: 200–700 m width: 50–540 m	Massive, disseminated, veinlet	VHMS deposit	Yang et al. (2000)
Sandashan (54)	Jinghong, Yunnan	100°50′ 22°02′	Cu	Cu: 0.2 Mt	Cu: 0.5%	Triassic post-collision crustal extension environment	Bimodal suite: felsic volcanic rocks	Silicification, sericitization, chloritization	Chalcopyrite, pyrite, pyrrhotite	Orebody: length: 50–500 m thickness: 1–12 m	Lenticular	VHMS deposit	Yang et al. (2000)

metallogenic belts in the world (i.e., Tethyan, Palaeo-Asian, Circum-Pacific). The STMD is characterized by its unique tectonic setting, a variety of mineralization styles, and complicated deposit types with immense prospectivity. The STMD contains a number of giant deposits discovered in the 1960–80s (Table 1), such as the Yulong Cu deposit (Rui et al., 1984; Ma, 1990; Hou et al., 2001a), Gacun Zn–Pb–Cu deposit (Xu et al., 1993; Hou et al., 1999, 2001b), Jinding Pb–Zn deposit (Ye et al., 1992), Ailaoshan Au deposit (Hu et al., 1995) and Lailishan Sn deposit (Liu et al., 1993), and recently discovered large deposits such as Xiasai Ag deposit, Baiyangping Ag deposit, Gala Au deposit, and Yagra Cu deposit. The metallogensis in the STMD is closely related to the development of the Sanjiang Tethys (Liu et al., 1993; Li et al., 1999). Since the 1960s, a large number of papers on the geology and ore deposits in the Sanjiang Tethys have been published in the Chinese literature, but none describe the relationship between this orogen and metallogenic relations, nor explain why these different orogens display differing metallogenic characteristics with some orogens apparently more mineralized than others (Richard, 1999). This paper describes the mineralization characteristics and deposit types of the main metallogenic provinces in the STMD, and analyses the tectonic settings and environments under which these deposits formed, based on the data from our present, as well as previous, studies on the Sanjiang Tethys in southwestern China.

2. Regional geology and tectonic history

The STMD, with an area of about 160,000 km^2 (Liu et al., 1993), forms a significant part of the giant Tethyan metallogenic domain. Tectonically, it is located in the Sanjiang Palaeo-Tethys, which is in the southeast segment of the East Tethyan tectonic domain, east of the Himalayan–Tibetan Orogen (Fig. 1). The complex geological and tectonic history of the STMD is due to subduction of the Tethyan Ocean slab, subsequent arc orogeny by arc-continent collision during the Palaeozoic–Mesozoic period, and continent–continent collision during the Himalayan period (Fig. 1; Yin and Harrison, 2000).

Reconstruction of tectonic history and sedimentary formations reveals that, during the Early Palaeozoic, the East Tethyan tectonic domain in SW China was composed of a Proto-Tethyan Ocean and scattered Pan-Cathaysian continental blocks (Pan et al., 1997; Li et al., 1999). Based on the Palaeo-ophiolitic sutures, there are four oceanic branches for the Proto-Tethyan Ocean: 1) the Palaeo-Asian Ocean separated from the Eurasian Continent, 2) the Qinling–Qilian–Kunlun Ocean (AKMS), 3) the Palaeo-Jinshajiang Ocean and 4) the Palaeo-Lancangjiang Ocean separated from the Gondwana Continent (Pan et al., 1997). By the end of the Early Palaeozoic, the South China Ocean collided with the Palaeo-Jinshajiang Ocean to become a continental mountain belt (Ren, 1987; Liu, 1993; Yan and Geng, 1993), while the Qinling–Qilian–Kunlun Ocean closed to form a subduction-related mountain system (Hao et al., 1983; Zhang, 1988). Also, the Palaeo-Jinshajiang Ocean probably became a marginal foreland basin (Li and Liu, 1991). Scattered continental blocks, such as the Yangtze (South China), Sino-Korean, Qaidam, Tarim and Changdu–Simao blocks, were united to form the unified pan-Cathaysian continental block in the remaining Palaeo-Asian Ocean and Songpan–Garze Ocean (Liu et al., 1993; Pan et al., 1997; Li et al., 1999).

The Late Palaeozoic was the main period during which the pan-Cathaysian continent break-up took place and the Palaeo-Tethys began to develop (Li et al., 1999). The opening of the Jinshajiang Ocean (JS) during the Palaeozoic (361.6 to 269.1 Ma; Zhan et al., 1998; Wang et al., 1999b) resulted in the separation of the Changdu–Simao block from the Yangtze block (Huang and Chen, 1987; Li and Liu, 1991; Liu et al., 1993). The Palaeo-Lancangjiang Ocean (LS) continued its development and further separated from the Gandwana Continent during this period (Hou et al., 1996a,b). Both the Jinshajiang and Lancangjiang Oceans were subducted beneath the Changdu–Simao block at the Early Permian and subsequently resulted in the formation of continental margin arcs along the block (Fig. 2; Liu et al., 1993; Mo et al., 1993), which now comprise part of the Qiangtang terrane (Fig. 1). The Garze–Litang oceanic basin separated along the western margin of the Yangtze in the Permian, and was marked by the ophiolite mélange zone (GLS) (Fig. 2; Hou et al., 1983, 1995). Westward subduction of the oceanic slab resulted in the Late Triassic Yidun island-arc (Figs. 1 and 2; Hou, 1993; Hou et al., 1995, 2001a). The Songpan–Garze Ocean was widely filled by the Triassic thick flysch complex (Yin and Harrison, 2000).

The continental block group formed in the Late Palaeozoic was again dismembered at the end of the Late Triassic, and the Meso-Tethys then appeared (Huang and Chen, 1987; Liu et al., 1993; Li et al., 1999). In the East Tethys tectonic domain, the Meso-Tethys has two ocean branches with different timing and size: Bangong Ocean (BNS) between the Qiangtang and Lhasa terranes, and Yalung Zambo Ocean (IYS)

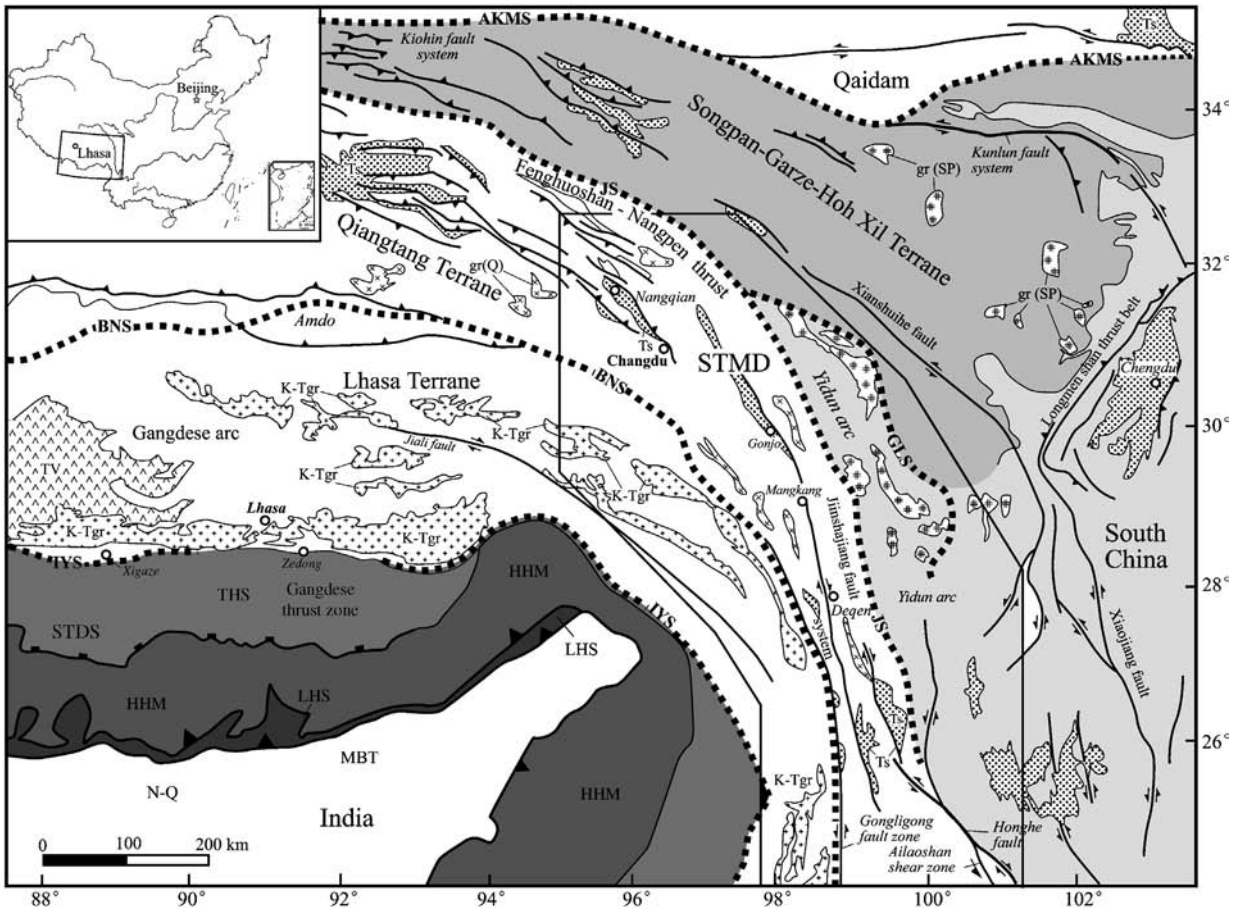

Fig. 1. Simplified tectonic map of the Himalayan–Tibetan Orogen (after Yin and Harrison, 2000). (1) Major rock and tectonic units: N–Q—Late Tertiary–Quaternary sediments; Ts—Tertiary sedimentary rocks; Tv—Early Tertiary volcanic rocks in Lahsa terrane; THS—Tethyan Himalayan sequences; HHM—High Himalayan metamorphic rocks; LHS—Low-Himalayan meta-sedimentary sequence; (2) Major plutons: K–Tgr—Gangdese granite batholith; gr(Q)—Miocene plutons in Qiangtang terrane; gr (sp)—Miocene plutons in Songpan–Ganze–Hoh Xil terrane; gr (YD)—Late Triassic plutons in Yidun arc; (3) Major suture zones: IYS—Indian river–Yalu–Zangbo suture zone; BNS—Bangonghu–Nujiang suture zone; JS—Jinshajiang suture zone; AKMS—Animaqing–Kunlun–Muzitage suture zone; GLS—Ganze–Litang suture zone; (4) Major Cenozoic Structures: STDS—South Tibetan detachment system; MCT—Main central thrust fault; MBT—Main boundary thrust fault.

between the Lhasa terrane and the Tethyan Himalaya (Fig. 1). The Gangdese block or Lhasa terrane between these two oceans corresponds to Sengor's Cimmerian continent (Hao et al., 1983; Sengor, 1989), and connects eastward with the Chayu–Lianghe block in eastern Tibet, where Late Yanshanian–Himalayan granitoids are strongly developed (Fig. 2). The Bangong Ocean was opened around the Jurassic (Yin and Harrison, 2000) and produced a well-developed ophiolite suite. The Yalung Zambo Ocean, corresponding to the Neo-Tethys proposed by Sengor (1989), opened around the Cretaceous (Xiao, 1983), and its northward subduction resulted in the formation of the Gangdese magmatic arc (Fig. 1; Allegre et al., 1984; Harrsion et al., 1992). With the Indo-Asian continent collision since the Palaeocene, a series of strike-slip fault systems, pull-apart basins, thrust systems, nappe structures and huge alkaline igneous belts were formed in the Sanjiang Tethys, a giant area of the eastern segment of the Himalayan–Tibetan Orogen (Fig. 1; Yin and Harrison, 2000).

3. Major metallogenic belts

A number of significant metallogenic belts in the STMD were formed in a series of major tectonic units (Fig. 2), such as 1) strike-slip fault systems, 2) thrust–nappe belts, and 3) intra-arc or rifting basins, in which a large number of giant ore deposits of precious metals (Au and Ag), base metals (Cu, Pb and Zn) and rare metals (Rb, Cs, Li, Ta and Y) were formed (Table 1).

3.1. The Ailaoshan gold belt

The Ailaoshan gold belt, 120 km long and 500–5000 m wide, is the most important in the STMD (Fig. 3). Four large (Laowangzhai, Dongguolin, Jinchang and Daping deposits), eight medium and numerous small gold deposits have been discovered in this belt. The cumulative reserves are more than 150 tonnes and prospective resources about 500 tonnes for the belt (Li et al., 1999). This metallogenic belt is largely distributed

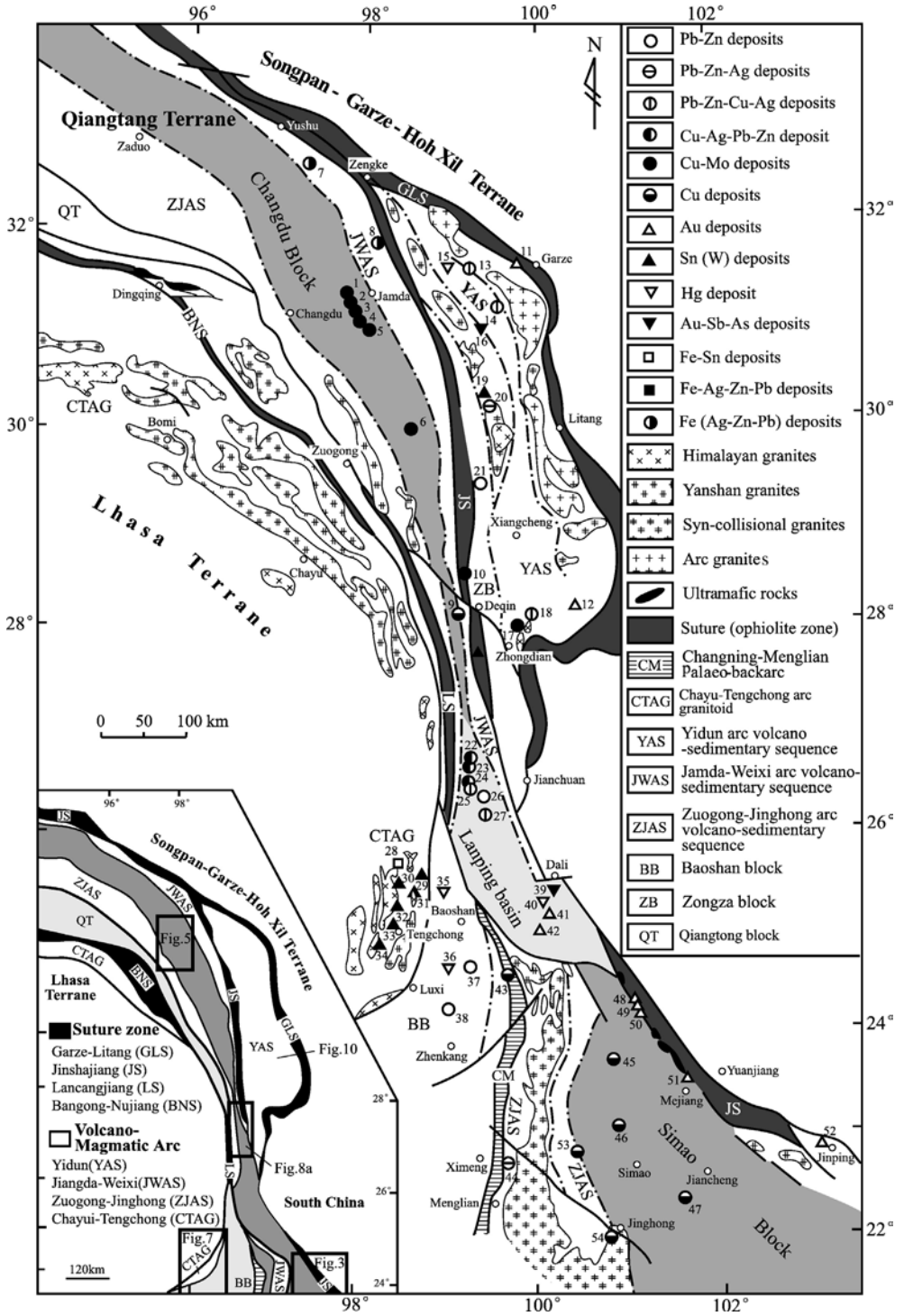

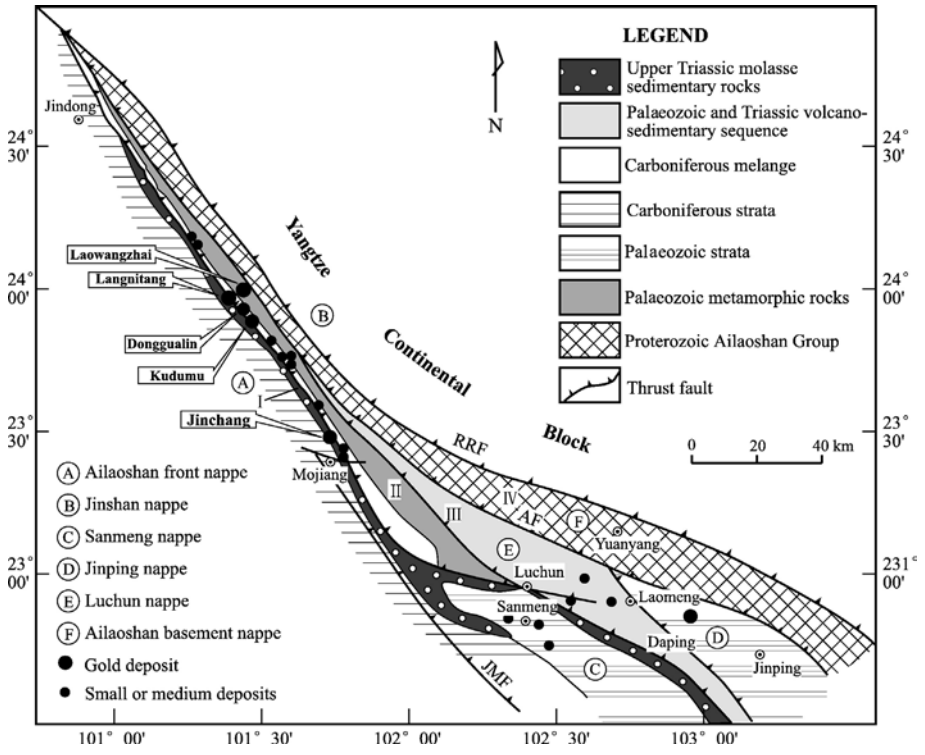

Fig. 3. The sketch geological map of the Ailaoshan Au ore belt (modified from Li and Liu, 1991). I—Foreland molasse formation; II—Front thrust zone; III—Central thrust zone; IV—Back thrust zone.

along the Jinshajiang (Ailaoshan) suture and is controlled by a complicated thrust–nappe belt formed by the Indian–Asian continent collision since the Palaeocene (Fig. 3).

Three secondary tectonic units have been identified across the thrust–nappe belt. The first is a high-grade metamorphic belt located between the Red River Fault (RRF) and the Ailaoshan Fault (AF). This belt consists of metamorphic rocks of the Proterozoic Ailaoshan Group (Tapponnier et al., 1990) and occurs as a nappe resulting from the westward thrusting of the Yangtze continent block. The second tectonic unit is a low-grade metamorphic belt located between the AF and the Jiujia–Mojiang Fault (JMF). This is composed of several large dextral *en echelon* nappes and structural slabs. These nappes or slabs, as the relicts of the Palaeozoic Ailaoshan oceanic crust and ophiolite mélange, are major ore-bearing formations, among which the Ailaoshan nappe hosts most of the large gold deposits and has the highest ore potential (Fig. 3). The third unit, the foreland molasse belt which occurs to the west of the JMF, forms as a marginal depression zone composed of a suite of molasse-like purplish red sandy conglomerates.

Tectonically, both the NW-trending AF and JMF constrain the distribution of the Ailaoshan gold belt, whereas the intersections of NW-striking brittle shear zones and nearly E–W-striking thrust faults control the spatial–temporal localization of the gold fields and gold deposits (Fig. 3). Individual deposits or orebodies normally occur in lithologically different brittle–ductile shear zones (Hu et al., 1995). They are mainly

Fig. 2. Simplified geological map showing tectonic framework of the Sanjiang Tethys and the distribution of significant ore deposits in the STMD (modified from Liu et al., 1993). Major suture zones: GLS—Garze–Litang suture zone; JS—Jinshajiang suture zone; LS—Lancangjiang suture zone; BNS—Bangong–Nujiang suture zone. Name and number of the large and medium-sized deposits: 1—Yulong; 2—Mangzong; 3—Zhanaga; 4—Duoxiasongduo; 5—Malasongduo; 6—Mamupu; 7—Zhaokalong; 8—Jiaduoling; 9—Luchun; 10—Yargla; 11—Gala; 12—Erze; 13—Gayiqiong; 14—Gacun; 15—Kongmasi; 16—Nongduke; 17—Xuejiping; 18—Hongshan; 19—Cuomolong; 20—Xiasai; 21—Najiaoxi; 22—Baiyangping; 23—Fulongchang; 24—Yanzidong; 25—Huishan; 26—Jinding; 27—Baiyangchang; 28—Diantan; 29—Datongchang; 30—Xiaolonghe; 31—Gudong; 32—Tieyaoshan; 33—Laopingshan; 34—Lailishan; 35—Shuiyinchang; 36—Caopo; 37—Dongshan; 38—Mengxing; 39—Shihuangchang; 40—Maanshan; 41—Zhacun; 42—Bijiashan; 43—Tongchangjie; 44—Laochang; 45—Denghaishan; 46—Bailong; 47—Yaojiashan; 48—Laowangzhai; 49—Donggualin; 50—Lannitang; 51—Jinchang; 52—Daping; 53—Dapingzhang; 54—Sandashan.

hosted in ophiolitic sequence consisting of mafic–ultramafic rocks, carbonaceous basaltic tuff and tuffaceous rocks, with minor clastic rocks, crystalline limestone and radiolarian siliceous rocks. Some gold deposits are associated with the Himalayan lamprophyre and granodiorite-porphyries that intruded the ophiolite mélange, suggesting a genetic relation between them (Huang et al., 1997). Dating of the ore-bearing host rocks and altered wall rocks indicate that most of the gold deposits in the belt were formed mainly in the Himalayan epoch, although they show a much wider age range varying from 96 Ma to 28 Ma (Liu et al., 1993; Hu et al., 1995; Huang and Wang, 1996; Huang et al., 1997).

Based on gold-bearing formations and ore types, gold deposits in the Ailaoshan belt are divided into three styles: the Laowangzhai-style, Jinchang-style and Kudumu-style. The Laowangzhai-style deposits occur directly in the Lower Carbonaceous highly-pyritized, dolomitized and sericitized basaltic lava, breccia and tuffite, as well as quartz graywacke and sericitic slate. The orebodies occur as veins, irregular, lenticular bodies and, in places, stratabound lenses (Fig. 4). The Kudumu-style deposits occur in pyritized and sericitized tuff and sheared basaltic lavas of Middle Carbonaceous age. The orebodies are generally stratabound, pod-like or occur in veins. The Jinchang-style deposits occur mainly in the contact zones between highly silicified and carbonatized ultramafic rocks and volcano-sedimentary sequences, and the orebodies are mostly lenticular and stratabound veins. Gold-bearing quartz veins and lenses commonly occur in fault or fracture zones; whereas stratabound and lenticular gold-bearing orebodies are hosted in quartz graywacke and also occur in contact zones of metasomatized mafic–ultramafic rocks (Hu et al., 1995).

Fluid inclusion data for these gold deposits show that the homogenization temperature of the ore-forming fluids ranges from 280 °C to 110 °C, yielding estimated ore-formation pressures between 720 and 400×10^6 Pa (Liu et al., 1993; Hu et al., 1995). The $\delta^{34}S$ values of ten samples from the ore-bearing altered rocks and pyrite are between −8.38‰ and 5.07‰ with an average of 0.82‰, suggesting that the sulphur in the wall rocks was mantle-derived (Hu et al., 1995). The $\delta^{34}S$ values of 52 sulphide samples vary from −2.37 to 3.60‰ with an average of 0.60‰, indicating that the ore sulphur in the sulphides probably comes from wall rocks or deep mantle sources (Hu et al., 1995). Based on the δD–$\delta^{18}O$ data for gangue quartz from three gold deposits, the homogenization temperatures, hydrogen and oxygen isotope values for the ore-forming hydrothermal fluids were estimated to be in the range between δD values of −95.8 and −33.1‰ for and $\delta^{18}O$ values of −2.08 and 8.8‰ (Hu et al., 1995), suggesting a mixing of ore-forming fluids of magmatic and meteoric origins. Magmatic water is dominant in the ore-forming fluid for the Jinchang-style deposits, whereas meteoric water is dominant for the Laowangzhai-style deposits (Hu et al., 1995). Recent systematic study of He–Ne–Ar isotopes suggests a contribution of mantle fluids to the hydrothermal system (Huang and Wang, 1996).

3.2. Yulong porphyry copper belt

The Yulong porphyry copper belt, the most important belt of its type in China, is tectonically located in the

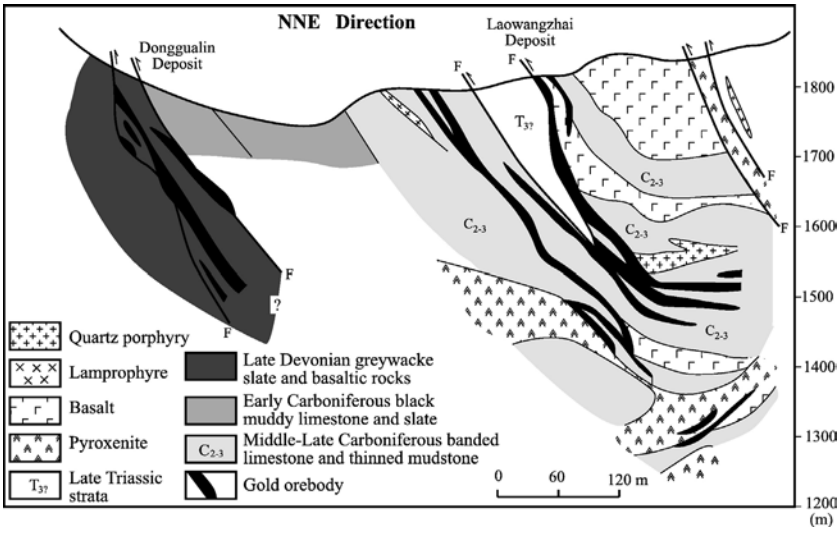

Fig. 4. A simplified geological cross-section in the Laowangzhai gold ore district in the Ailaoshan gold belt (modified from Liu et al., 1993).

Changdu–Simao continental block. It was mainly distributed around the Cenozoic uplift between the Gonjo and the Nanqen strike-slip pull-apart basins, filled up with Tertiary red molasse accumulations more than 4000 m thick, and alkaline volcanic rocks with K–Ar ages varying from 37.5 to 42.4 Ma (Zhang and Xie, 1997; Wang et al., 2000a,b; Fig. 5). The chronologic data indicate that the magmatism of the Yulong porphyry belt has at least three stages, early, middle and late stages, corresponding to magmatic peaks around 52, 41 and 33 Ma, respectively (Ma, 1990; Hou et al., 2003a). The emplacement of the porphyries was strictly controlled by a large-scale strike-slip fault system produced by the Indian–Asian continental collision initiated in the Palaeocene (Fig. 5; Li and Liu, 1991; Liu et al., 1993; Hou et al., 2003a). The right-lateral shearing along the fault system yielded a set of associated sinistral NW–NNW-trending *en echelon* folds and compression-shear faults, which are intersected by the strike-slip faults at acute angles (Fig. 5), and controlled the emplacement of the porphyries and formation of the Yulong copper belt.

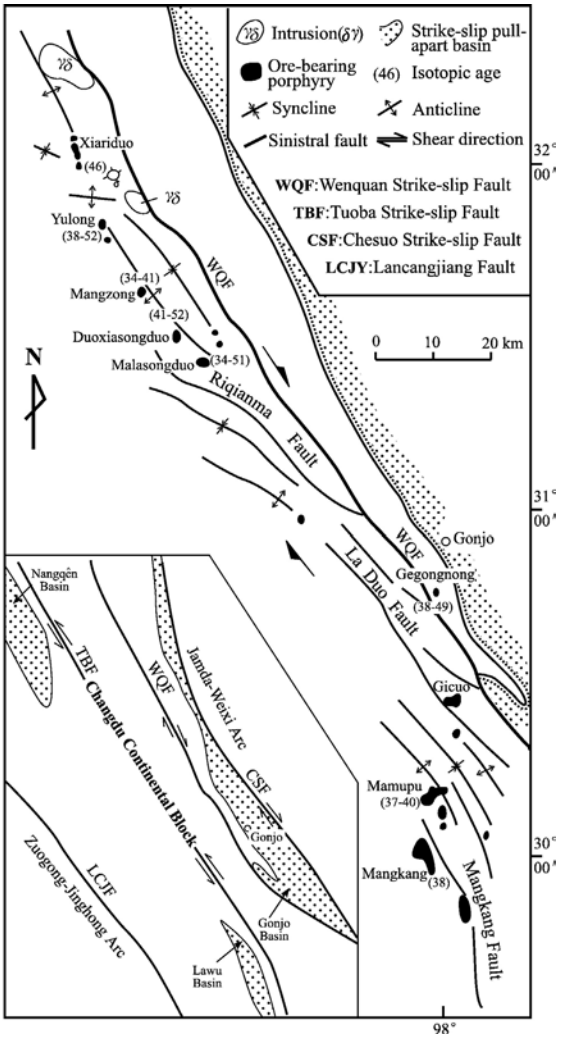

Fig. 5. Structural features and porphyry distribution in the Yulong porphyry Cu belt, eastern Tibet (after Liu et al., 1993; Hou et al., 2003a). The Yulong ore-bearing porphyry belt is mainly controlled by a set of the secondary NNW-directed sinistral strike-slip faults and folds derived from the Wenquan strike-slip fault; the boxed area in the left–lower corner in the figure shows the Jinshajiang strike-slip fault system consisting of a series of strike-slip faults, such as the Chesuo, Wenquan and Tuoba Faults. These faults resulted in the formation of the strike-slip pull-apart basins such as Gonjo, Nangqen and Lawu basins.

The Yulong porphyry copper belt is over 200 km long and 15−30 km wide, and composed of more than 20 monzonitic granite-porphyry bodies (Fig. 5). Most of the bodies in the belt intruded Triassic strata, were commonly emplaced at shallow depths (1.5−3 km), and dip steeply as vertical pipes or stocks (Fig. 6). The ore-bearing porphyries are characterized by a high potassium content, belonging to high-K calc-alkaline and shoshonitic series (Zhang et al., 1998b). The rocks are rich in LILE (K, Rb and Ba) and depleted in HFSE (Zr, Hf, Nb and Ta), and have LREE-enriched patterns (Zhang et al., 1998c, 2000; Hou et al., 2003a). Sr–Nd isotopic compositions suggest that the felsic magmas were derived from the mixing of subducted Jinshajiang oceanic slab-derived melt with hydrous enriched mantle-derived melt (Hou et al., 2003b). Although such ore-bearing porphyries occur in a continent–continent collisional orogen, the mineralization features are similar to those of the porphyry copper ores in the Andean belt, which results from an oceanic–continental collision (Camus and Dilles, 2001).

Ore-bearing porphyry and wall rocks have suffered from strong hydrothermal alteration. Alteration zonation, from the core of the orebody outwards to the wall rocks, ranges from a potassic silicified zone through a quartz sericite zone and argillization zone to a propylitization zone. The potassic–silicified zone is mainly developed inside the porphyry bodies, and is marked by large amounts of secondary potassic feldspar and quartz. The quartz sericite zone is in the periphery of a body, appearing mainly inside the porphyries and the contact zone and superimposed on the potassic–silicified zone. This zone is characterized by sericitization with large amounts of chlorite, epidote and tourmaline. An argillization zone was only developed in the Yulong deposit, and is characterized by the occurrence of quartz and clay minerals (illite and kaolinite). The propylitization zone is common in the surrounding strata and developed around the quartz

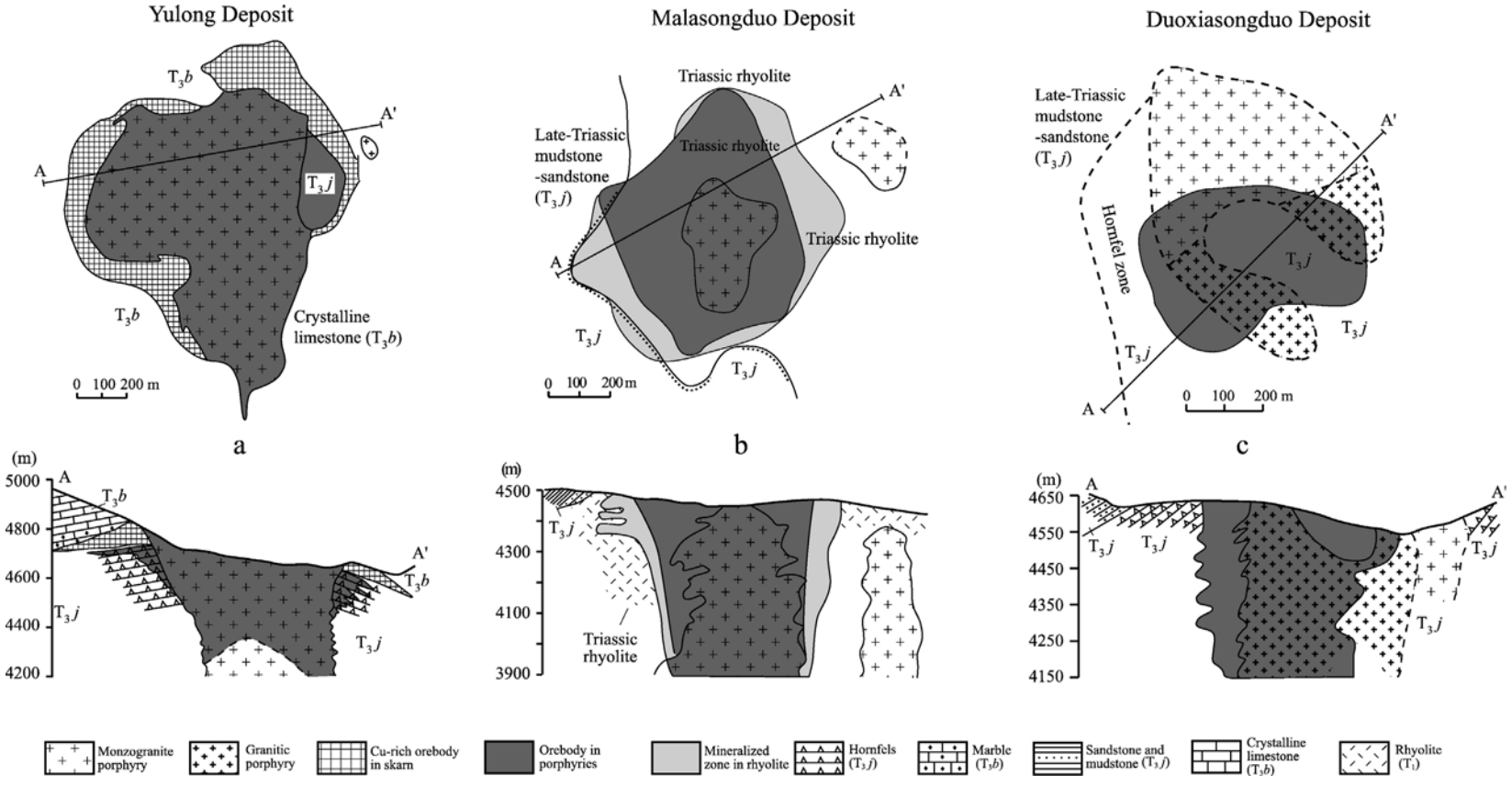

Fig. 6. Plan map and cross-section of hydrothermal mineralization and alteration of Cu deposits from the Yulong porphyry Cu belt (after Hou et al., 2003a).

sericite zone. The features of the protolith are well-preserved despite the low-to-moderate-temperature hydrothermal alteration.

Three forms of mineralization are present: (1) disseminated to semi-massive mineralization in the core of the porphyry bodies; (2) steeply-dipping or vertical orebodies along contact zones between porphyry intrusions and host rocks; and (3) layered or lenticular ore lenses in altered host rocks. These styles of mineralization are commonly spatially related and occur as concentric zones surrounding an inner core of the porphyry. Most of the porphyries are weakly mineralized except for their central parts that contain high-grade disseminated and veinlet-type Cu and Mo ore with pyrite + chalcopyrite + molybdenite assemblages. The contact zones are characterized by veinlets, lenticular, semi-massive to disseminated Cu–Fe polymetallic mineralization with assemblages of pyrite + chalcopyrite + magnetite ± molybdenite ± bismuthinite ± ilmenite ± galena ± sphalerite. Vein-like, layered and lenticular Pb, Zn, Ag and Au mineralization occurs in altered host rocks and has an assemblage of pyrite + chalcopyrite + galena + sphalerite.

According to Li et al. (1981) and Rui et al. (1984), the mineralizing process can be divided into three stages: (1) a pneumatolytic stage, with ore-forming temperatures from 400 °C to 700 °C, in which the porphyry was largely subjected to potassic alteration and silicification, and the host rocks in the contact zones were transformed to skarn along with Cu–Mo mineralization; (2) a high-to-moderate temperature stage, with ore-forming temperatures from 200 °C to 500 °C, characterized by sericitization associated with Cu–Mo–Fe mineralization; and (3) a low-to-moderate hydrothermal stage, with ore-forming temperatures lower than 230 °C, in which argillization and propylitization are developed in the contact zones and the surrounding host strata associated with Au–Ag-polymetallic mineralization.

3.3. Tengchong–Lianghe tin and rare metal belt

The Tengchong–Lianghe metallogenic belt is located in the eastern segment of the Gangdese magmatic arc and occurs in the Chayu–Tengchong granite belt (Fig. 2). It is composed of two large tin deposits (Xiaolonghe and Lailishan), one large rare metal deposit (Baihuanao) and five medium-sized tin deposits in addition to nearly a hundred mineralized occurrences. This belt is also an important tin-polymetallic and rare metallic belt in the STMD (Fig. 7). The southern segment of the Tengchong–Lianghe belt is connected with the Southeast Asian tin belt, and thus is a part of the 8000 km long giant tin belt. There are various genetic types of the tin deposits in the belt. More than thirty elements are recorded in the rare metal deposits. Of them, the reserve of Rb is significant, accounting for one third of the world's total Rb reserves (Li et al., 1999). Significant amounts of elements such as Cs, Li, Ta, Sc, Y, Sn and W are also present.

At least three N–S trending granitoid Groups have been recognized in the tin–rare metal belt: the Early Cretaceous Donghe granitoid Group; the Late Cretaceous Jiyong granitoid Group; and the Early Tertiary Binlangjiang granitoid Group (Fig. 7). The Early Cretaceous granitoid Group is divided into three major units (Qipanshi, Mingguang and Diantan), and has an emplacement age varying from 100 Ma to 143 Ma as determined by K–Ar dating methods (Liu et al., 1993; Chen, 1987). The granitoids mainly consist of granodiorite and granite, and are mostly mineralized. The two mineralization types found are the skarn-type and vein-type cassiterite–sulphide deposits. The former occurs at the outer contact zone between granitoid and wallrock, and the latter occurs in the inner contact zone, associated with strong silicification, sericitization, chloritization and pyritization.

The Late Cretaceous Jiyong granitoid Group is composed of major ore-bearing intrusions, and includes four major granitoid units (Qingcaoling, Yunfengshan Xiaolonghe and Yongjinggong) with a limited K–Ar age range of 80–78 Ma (Chen, 1987; Liu et al., 1993). Ore-bearing granitoids are mainly monzonitic granite and K-feldspar granite with abundant alkalis and volatile components (F, H_2O) and a high abundance in LILE and ore elements. The greisen- and skarn-types are the main types of tin mineralizations. A spectrum of veined greisen, planar greisen and greisenized tin deposits occur in the inner contact zones, whereas skarn-type tin and tungsten mineralizations are developed in the outer contact zones. A combination of both mineralization types normally results in the formation of larger-sized tin deposits, such as the Xiaolonghe tin deposit, which is composed of veined, greisen-type ores and subordinate skarn-type ores.

The Early Tertiary Binlangjiang granitoid Group consists of the Xinqi, Lailishan and Baihuanao units (Fig. 7), whose K–Ar ages vary between 51.1 and 59.8 Ma (Chen, 1987; Liu et al., 1993). The Lailishan tin deposit, the largest in the STMD, occurs in biotite K-feldspar granites in the Lailishan granite unit, whereas the Baihuanao deposit, the largest rare metal deposit in the STMD, occurs in alkali-feldspar granites in the Baihuanao granite unit.

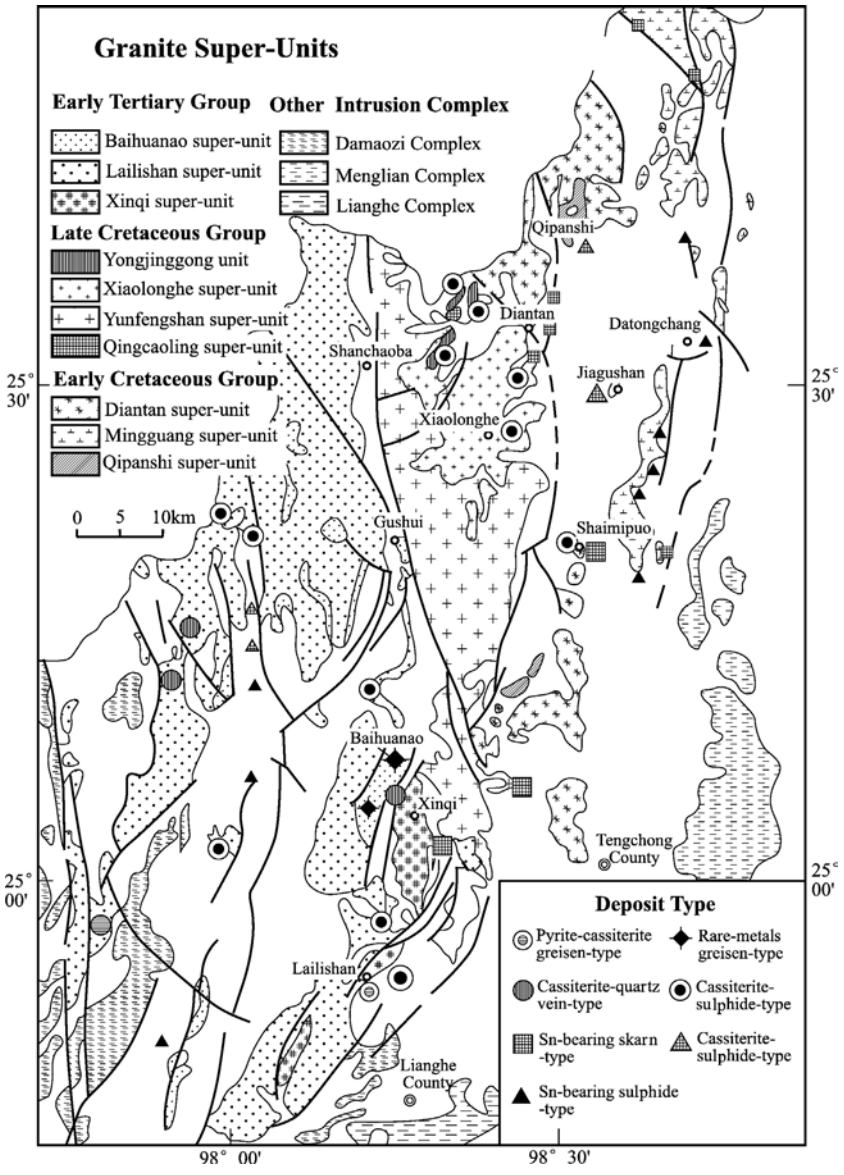

Fig. 7. Simplified geological map showing the distribution of the Early Cretaceous–Early Tertiary granitoid super-units and the related Sn and rare-metal deposits in the Tengchong–Lianghe metallogenic belt (modified from Chen, 1987).

The Lailishan granite is characterized by high K, F and S contents and high initial $^{87}Sr/^{87}Sr$ ratio (0.7124–0.7138), suggesting crustal anatexis (Lu and Wang, 1993). The Lailishan ore-bearing granites have a high Sn content, ranging from 150 to 200 ppm, Mg/Ti values between 1.5 and 3.0, and Zr/Sn values between 10 and 416, showing characteristics of tin-bearing granites (Lehman, 1990). The tin orebodies occur in the lower contact zones and the surrounding fractured zones of the granitic intrusion. The tin ore is of the greisen-type, and the grade ranges between 0.63% and 1.58% Sn (Liu et al., 1993). The host greisen consists of quartz, muscovite, topaz and fluorite, and accounts for 30–50% of the tin ore. Base metal sulphides are mainly composed of pyrite, pyrrhotite and lesser amounts of sphalerite and galena, occupying 30–60% of the tin ore.

The Baihuanao ore-bearing granites are mainly alkali-feldspar granites, characterized by a high SiO_2 and alkali (K_2O+Na_2O) content, and a high abundance of LILE (K, Rb, Cs and Li) and REE elements (Liu et al., 1993). Petrologic study indicates that these granitic magmas experienced a complex evolution from rare-earth-mineralized granite through Nb–Ta-mineralized granite to Sn–W-mineralized granite (Liu et al., 1993).

Disseminated and greisen-type ores are predominant in the Baihuanao deposits. Disseminated ore occurs in strongly greisenized and potassic-altered granites, whereas veined ore mainly occurs in linear greisen developed in the inner and outer contact zones of granites. There are much higher contents and a great variety of lithophile elements (Sn, W, Li, Rb, Cs, Nb Zr, Hf, Y, Ce, Sc, etc.) in the Baihuanao deposit.

3.4. Lanping zinc–lead–silver–copper polymetallic belt

The Lanping Zn–Pb–Cu–Ag polymetallic belt is tectonically located in the Lanping basin (Fig. 2), a large composite basin developed on the Changdu–Simao continental block. This basin experienced a complex evolutionary history, from Late Triassic–Early Jurassic intra-continental rifting, through Middle Jurassic–Cretaceous down-warping, and Himalayan strike-slip movement. One giant Pb–Zn deposit (Jinding), two large Ag deposits and three medium-sized Cu–Ag metallic deposits, as well as several smaller deposits occur in this basin (Li and Kyle, 1997; Jue, 1998; Wang and Yan, 1998), and form as an important polymetallic belt in the STMD (Figs. 2 and 8a). Based on the mineralization styles, host rocks and nature of ore-bearing sequences, at least four genetic types have been recognized: 1) exhalative-sedimentary type; 2) vein-type; 3) exhalative-replacement type; and 4) sedimentary-reformed type (Wang et al., 2000a).

The exhalative-sedimentary deposits include three Ag polymetallic deposits (Huishan, Yanzidong and Xiawuqu) and two large Sr deposits (Dongzhiyan and Hexi), that comprise a 15 km long sub-belt (Fig. 8a and b). These deposits commonly occur in the Upper Triassic Sanhedong Formation, which was formed during intra-continental rifting, and consist of siliceous rocks, laminated finely crystalline dolomite and dolomitic limestone. Petrographic and geochemical studies indicate that the host rocks (siliceous rocks and dolomite) are typical exhalative-sedimentary products (Wang et al., 2000a). The Ag polymetallic orebodies are normally stratabound or stratiform and, in places, lenticular. The ores are banded, brecciated, massive and disseminated, with galena, siderite, chalcopyrite and freibergite as major metallic minerals. Fluid inclusion data for these deposits show that the ore-formation temperatures ranged from 100 °C to 180°C and the fluid salinity was between 0.87 and 4.01 equiv. wt.% NaCl (Wang et al., 2000a). The $\delta^{34}S$ values of metallic sulphides range from −7.49 to 3.42‰ (Wang et al., 2000a), indicating that the ore S was not derived from seawater sulphate, but was probably formed by reduction of seawater sulphate by bacteria. Lead isotopic composition of the ore Pb suggests an upper crustal source (Wang et al., 2000a).

The vein-type Ag–Cu-polymetallic deposits mainly occur in Cretaceous strata in the Himalayan strike-slip basins, and are strictly controlled by nearly N–S-trending faults. Representative deposits are the Baiyangping, Fulongchang and Hetaojing deposits, which comprise a 45 km long Cu-rich sub-belt (Fig. 8b). The orebodies are mostly large veins or lenses and are hosted in the transitional zone between permeable medium- to coarse-grained sandstone and impermeable calcareous argillite. Sulphide ores are commonly brecciated, containing stockwork with cataclastic textures. Except for base metal sulphides, these ores commonly contain large amounts of sulfosalt minerals (e.g., tetrahedrite) bearing Cu, Ag, Bi, Co and Ni elements (Wang et al., 2000a). Chemical analysis of fluid inclusions shows that the ore-forming fluids had high contents of CO_2, CH_4 and organic matter. These fluids were rich not only in low-temperature element association (Pb–Ag–As–Sb), but also in high-temperature element association (Cu–Co–Ni–Bi), probably suggesting multiple sources of ore fluids. The $\delta^{34}S$ ratios of the metallic sulphides have a bimodal distribution (2.8‰ and 6.2‰), supporting this contention.

The exhalative-replacement deposits, exemplified by the giant Jinding Pb–Zn deposit, are controlled by N–S-striking Bijiang Fault, and occur in the Himalayan strike-slip basins (Fig. 8a). Two tectono-stratigraphic units are found in the Jinding district: the Palaeocene ore-bearing subaerial strata and the overlying reversed Upper Triassic–Middle Jurassic nappe (Fig. 9). The orebodies are favorably hosted in the middle succession of the Palaeocene Yunlong Formation. The host succession is composed of limestone breccia and slump breccia in the interlayered *decollement* zone and breccia-bearing quartz sandstone. The orebodies occur as stratified, lenticular and irregular lenses, parallel to the bedding of the strata. The footwall is a gypsum-bearing sandy and muddy siltstone acting as a confining bed against fluid migration and displaying celestite alteration, silicification and dolomitization. The hanging-wall is a Middle Jurassic–Cretaceous sandstone–mudstone nappe, acting as a barrier against fluid discharge, and affected by slight baritization and decolorization. There is distinct zonation from top to bottom, of anhydrite, celestite, pyrite, sphalerite + galena and cinnabar. The homogenization temperature of the fluid inclusions ranges from 145 °C to 310 °C and the salinity between 5.0 and 14.5 wt.% NaCl equiv. (Ye et

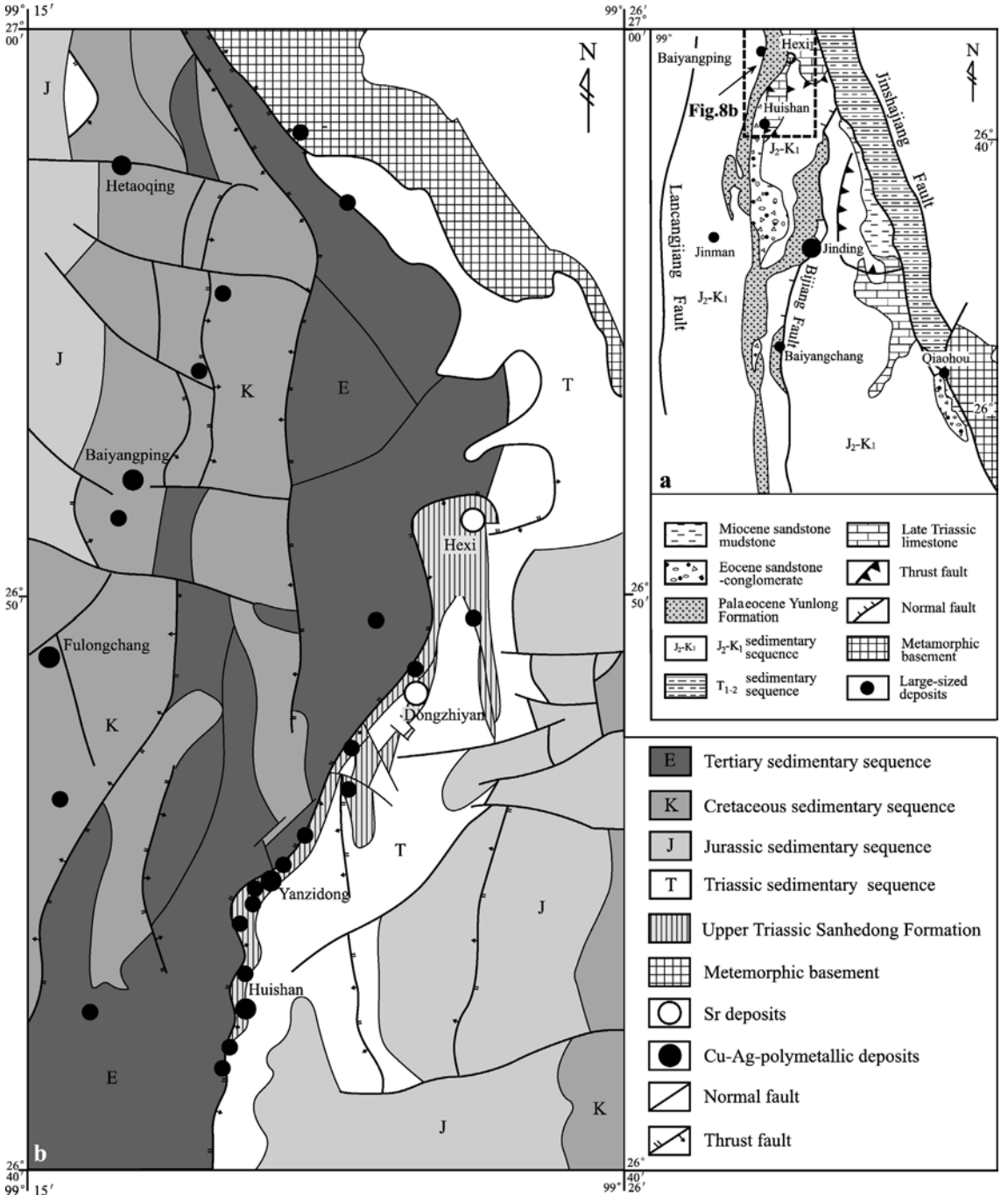

Fig. 8. Simplified geological map of the Ag-polymetallic mineralization belt in the Sanshan–Baiyangping area (modified from Wang et al., 2000a).

al., 1993). The ore-forming fluids might have been derived from pore fluids (brines) or mixed fluids in a deep-seated (magmatic ?) high-pressure fluid reservoir (Ye et al., 1993). Xue et al. (2000) recently reported $^{3}He/^{4}He$ ratios of sulphides (pyrite and sphalerite) and sulphate (barite) from the Jinding deposit, which range from 2.70×10^{-7} to 11.40×10^{-7}. The $^{3}He/^{4}He$ ratios of the Jinding deposit (0.19–0.82 Ra; $Ra=(^{3}He/^{4}He)_{atm}=1.40\times10^{-6}$) are higher than those of the crust (0.01–0.05 Ra) (Stuart et al., 1995; Hu et al., 1998), suggesting the contribution of minor mantle-derived fluid to the hydrothermal system (Xue et al., 2000). The $\delta^{34}S$ values of metallic sulphides in the deposit vary from −30.42 to 1.71‰, suggesting that sulphates were reduced by

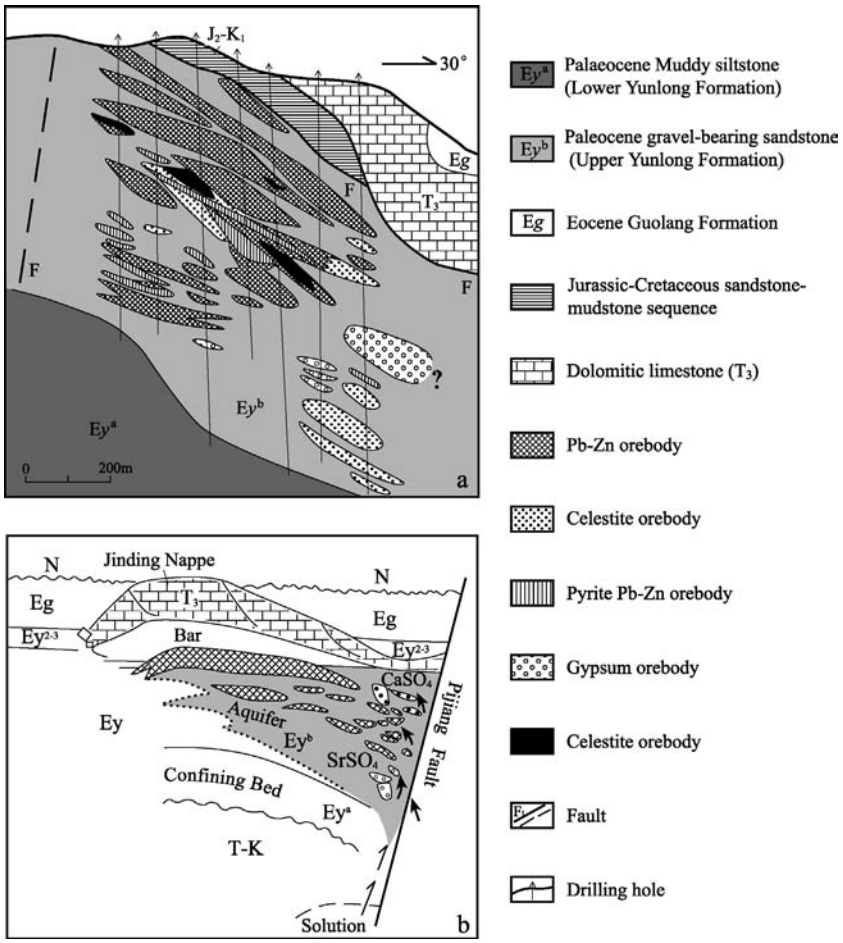

Fig. 9. Simplified geological section (a) and ideal model (b) of the Jingding Pb–Zn deposit in the Lanping basin (modified from Luo et al., 1994).

organic matter as the ore sulphur source (Ye et al., 1992).

The sedimentary-reformed (remobilized) type deposits are represented by the Baiyangchang Ag–Cu-polymetallic deposit and the Jinman Cu deposit (Fig. 8a). These deposits appear to have been controlled by a host sequence that occurs between permeable limestone and the overlying impermeable argillite, in the lower part of the Middle Jurassic strata. The orebodies form as large veins, or are stratabound with banded, brecciated, massive or veined-stockwork. The major metallic minerals include tennantite, chalcopyrite, bornite, freibergite, pyrite and argentite. Detailed ore textural studies indicate that the deposits were formed by two processes: primary metal enrichment initiated in the Jurassic–Cretaceous periods, overprinted by hydrothermal processes during Himalayan magmatism. Lead isotopic data from sulphides of both deposits yielded two Pb-model ages, ranging between 110 Ma and 165 Ma, and between 30 Ma and 70 Ma, respectively (Xiao and Chen, 1991; Chen, 1994; Wang and Yan, 1998). These ages correspond to those of two ore-forming processes. Fluid inclusion data show that the formation temperatures in the sedimentary stage were between 100 °C and 180 °C, whereas those in the hydrothermal reformed stage were between 200 °C and 290 °C (Ye et al., 1993). The $\delta^{34}S$ ratios of galena and sphalerite vary mostly from −20.4 to −3.9‰, suggesting an organic source for the ore S in the sedimentary metallogenic stage. The $\delta^{34}S$ values of chalcopyrite and tetrahedrite vary mostly around 0.0‰, suggesting magmatic sulphur as the ore sulphur source in the reformed stage (Chen, 1994; Wang and Yan, 1998; Wang et al., 2000a).

3.5. Baiyu–Zhongdian polymetallic belt

The Baiyu–Zhongdian belt is an important polymetallic belt in the STMD. Tectonically, this belt is located in the Late Triassic Yidun island-arc, which

resulted from westward subduction of the Garze–Litang oceanic Plate, and is composed of four metallogenic sub-belts, which were formed in different stages of evolution and have different extents (Figs. 2 and 10).

3.5.1. VHMS sub-belt

The volcanic-hosted massive sulphide (VHMS) sub-belt, including a large (Gacun), three medium (Gayiqiong, Shengmolong and Ronggong) and several tens of smaller polymetallic deposits, occurs in an intra-arc rifting zone in the northern segment of the island-arc (Figs. 10 and 11). The intra-arc rifting zone that formed along the volcanic arc is characterized by the development of fault-bounded basins and associated bimodal volcanic suites and abyssal sedimentary rocks, and is tectonically similar to the back-arc Okinawa Trough (Letouzey and Kimura, 1986) and the Miocene back-arc basin in northwestern Japan (Cathles et al., 1983). Two spatially separated fault-bounded basins, the Zengke and Changtai basins (Fig. 11), have been recognized within the intra-arc rifting zone with the water depth about 800–1200 m (Hu et al., 1992). Almost all VHMS deposits in the sub-belt cluster in both basins (Fig. 10; Hou and Mo, 1993; Hou, 1993; Xu et al., 1993; Hou et al., 1995).

A bimodal volcanic suite in these basins is composed of mafic and felsic rocks hosting the massive sulphide orebodies. The mafic package overlies a 50–250 m thick sedimentary sequence, and was in turn overlain by the extensive succession of interbedded sandstone, siltstone, conglomerate and deeper marine phyllite and chert (Hou et al., 2001a). The mafic rocks include basaltic volcanic rocks and an associated dike swarm or dike complex. Felsic volcanic rocks, at least 1000 m thick, extend NNW for 60 km. At least two felsic volcanic units occur in faulted contact. The lower felsic unit, overlain by tuffaceous siltstone, limestone and phyllite, is massive and auto-brecciated dacite or dacitic rhyolite. The upper felsic unit is asymmetrically exposed on both flanks of an anticline with a NNW axial direction. The main host-rocks of these units are rhyolitic pyroclastic rocks. A 30–50 m thick exhalative sequence, consisting of chert, barite, jasper and dolomite (Hou et al., 2001a), constitutes a favorable horizon, or ore equivalent horizon, as suggested for most VHMS systems (e.g., Sangster, 1972; Franklin et al., 1981; Large, 1992), which occurs on the top of a rhyolitic volcanic pile and is closely associated with sulphide orebodies in the sub-belt (Hou et al., 2001a).

The VHMS deposits in the sub-belt shows the classic morphology of a stratiform polymetallic massive-sulphide lens underlain by a stringer or stockwork vein zone, as recognized for VHMS deposits in Canada, Japan and Australia (e.g., Sangster, 1972; Franklin et al., 1981; Large, 1992). The stringer–stockwork zone is hosted in a dacitic–rhyolitic volcanic pile, and is made up of a series of stringer, stockwork and disseminated orebodies, which are concordant beneath the massive sulphide zone. At Gacun, the stringer–stockwork orebody occurs in the rhyolitic tuffaceous breccia, and shows a blanket-like stratabound zone (Fig. 12). At Gayiqiong, the stockwork orebody occurs in a dacitic volcanic pile, and is pipe-like. Stringer–stockwork Cu–Pb–Zn ore is the predominant type, whereas massive pyrite occasionally occurs in the center of the stratabound stringer zone. The dominant ore minerals are pyrite, sphalerite, galena and chalcopyrite, with minor arsenopyrite, pyrrhotite and ilmenite. The massive sulphide zone occurs on the top of the dacitic–rhyolitic volcanic pile and is closely associated with exhalative rocks. The zone consists of Zn–Pb–Cu–Ag-rich massive sheets or banded lenses. At Gacun, massive black ore is dominant in the massive sulphide zone, but massive yellow ore has not been recorded. The massive sulphide sheets are associated with exhalative rock (barite and barite-chert) and constitute five sulphide–sulphate units, suggesting complex processes, for example, episodic venting of the submarine hydrothermal fluids on the seafloor and rapid accumulation of sulphides in the slope and depression (Hou et al., 2001a). At Gayiqiong, massive sulphide lenses are closely associated with chert, jasper and siderite, and display typical sedimentary structures, such as bedding, layering, lamination or graded cross-bedding structures (Hou et al., 1995).

3.5.2. Porphyry–skarn Cu polymetallic sub-belt

The porphyry–skarn Cu polymetallic sub-belt is located in the southern segment of the Yidun island-arc and occurs in the Zhongdian calc-alkaline volcano-magmatic complexes, which are composed of Late Triassic andesitic–dacitic volcanic rocks and associated shallow-level intrusions. These intrusions share magmatic arc affinities with calc-alkaline volcanic rocks (Hou et al., 1995), and occur as porphyries and stocks. Ore-bearing intrusions are commonly porphyries of quartz diorite, quartz monzonite, and monzonitic granite. Dating of the ore-bearing porphyries yields a Rb–Sr isochron age range from 220 Ma to 240 Ma for the shallow-level emplacement of the felsic magmas (Liu et al., 1993), equivalent to or slightly later than arc volcanism in the area.

The ore-bearing porphyries in this belt have been subjected to strong hydrothermal alteration, and show

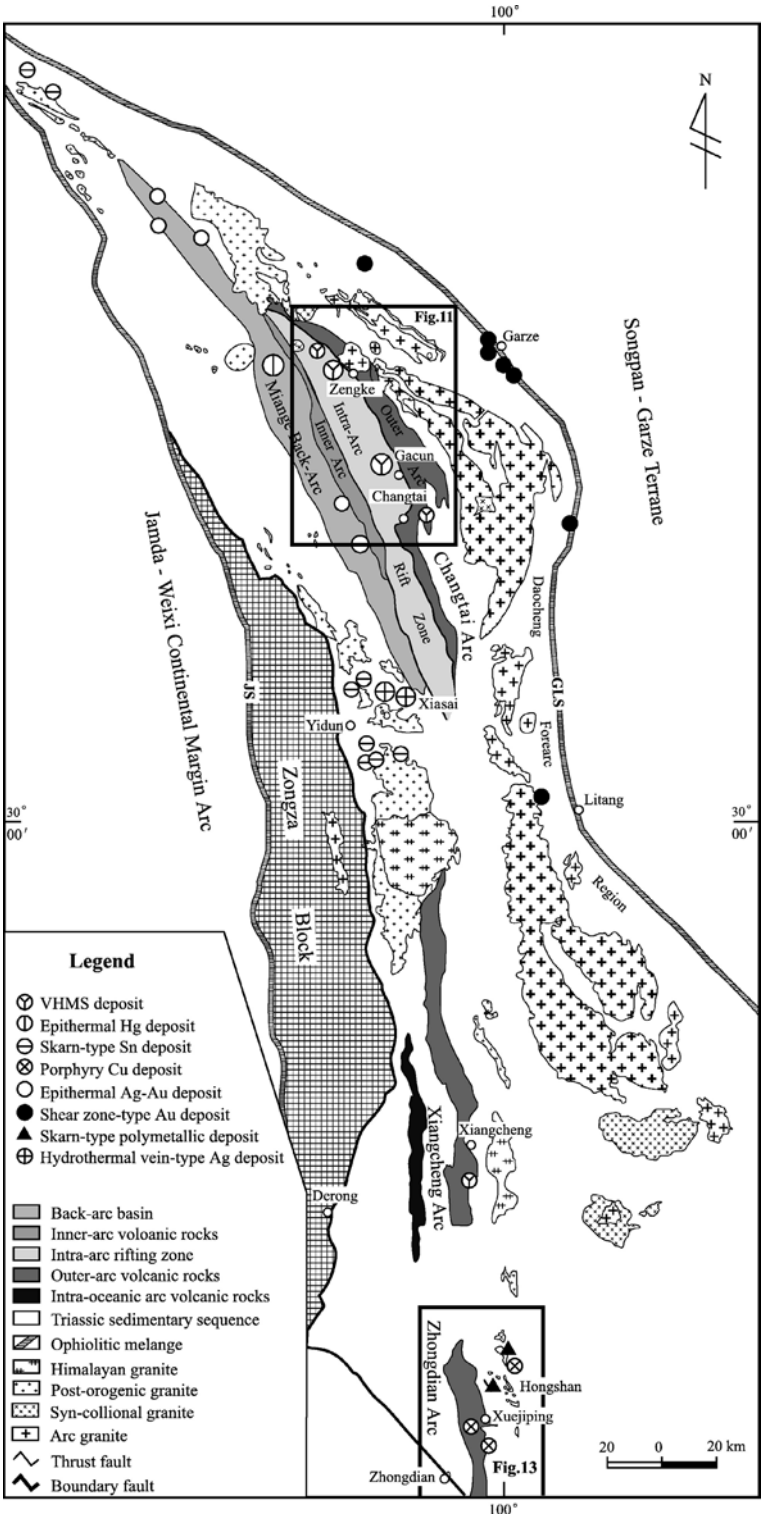

Fig. 10. Sketch map showing the tectonic framework of the Late Triassic Yidun island-arc and the distribution of polymetallic ore deposits in the Baiyu–Zhongdian metallogenic belt (Hou et al., 1995) GLS—Garze–Litang suture zone; JS—Jinshajiang suture zone.

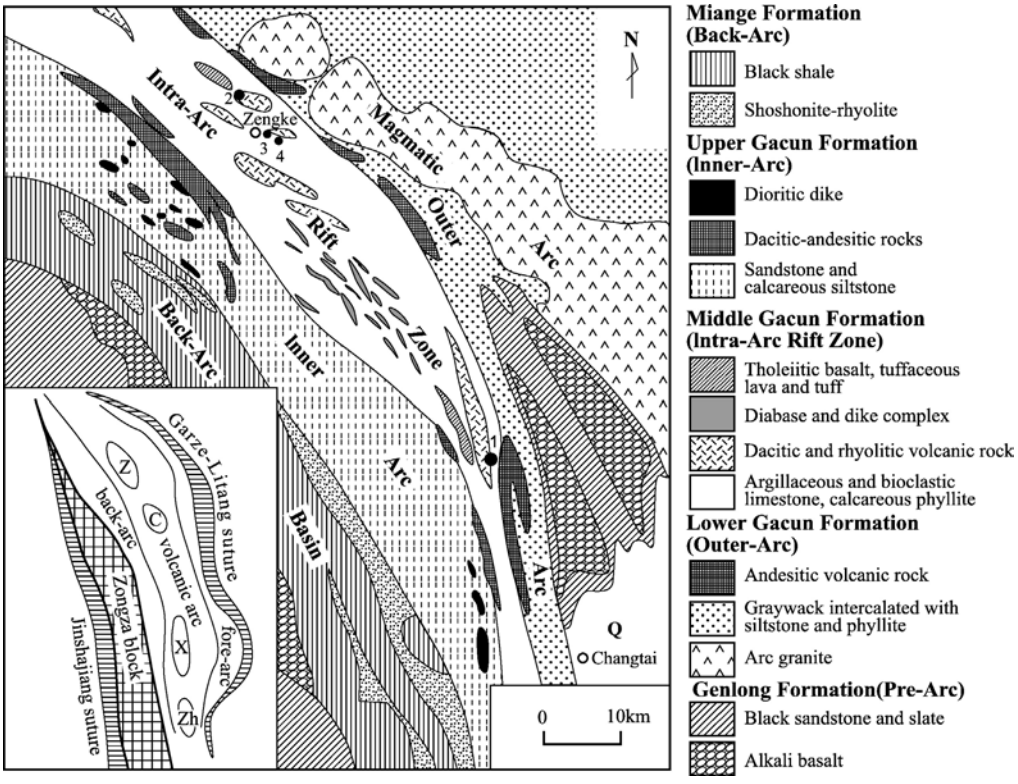

Fig. 11. Sketch map showing major tectonic units, volcano-sedimentary sequences and location of the VHMS deposits in the Changtai arc, northern segment of the Yidun island-arc (Hou et al., 2001a). GLS: Garze–Litang suture; JS: Jinshajiang suture; ZB: Zhongza block; Z. Zengke basin; C. Changtai basin; X. Xiangcheng basin; Zh. Zhongdian basin. 1: Gacun deposit; 2: Gayiqong deposit; 3: Ronghong deposit; 4: Kaigong deposit.

distinct alteration zonation from the core outwards: K-alteration zone (K-feldspar–sericite zone), quartz–sericite zone, carbonate alteration zone and propylitization zone. The Cu mineralization occurs mostly in the K-alteration zone and quartz–sericite zone and the orebodies are mainly disseminated, of stringer type or occur in veins. Representative porphyry Cu deposits include large Xuejiping deposit, and medium-sized Chundu and Lannitang deposits (Fig. 13).

A skarn is also developed along the contact zone between quartz monzonite and monzonitic granite porphyries and the overlying Triassic limestones, and the zone forms a 1.5 km long and 800 m wide skarn belt in the Zhongdian area. The skarn zones are commonly stratiform or stratabound and are major ore-bearing hosts for Cu-polymetallic mineralization. Diopside and grossular are the major skarn assemblages and occur as lenticular and stratiform bodies. The skarn also consists of minor magnetite, pyrrhotite, pyrite and chalcopyrite. The representative skarn-type deposits include the large Hongshan deposit and medium-sized Pulang and Gaochiping deposits (Fig. 13).

3.5.3. Sn–Ag-polymetallic sub-belt

The Sn–Ag-polymetallic sub-belt is 10–20 km wide and over 100 km long. This sub-belt is composed of a large Ag deposit (Xiasai), a medium-sized Sn–Ag deposit and numerous smaller Ag, Sn and polymetallic deposits and occurrences. It is located along the western margin of the Yidun arc, and stretches along the NNW-trending belt of A-type granites that were emplaced during the post-collision crustal extension period (Fig. 10; Hou et al., 2001b). These A-type granites, as a marker of orogenic collapse, have a wide K–Ar age range from 110 Ma to 70 Ma, but were mainly emplaced around 80 Ma (Hou et al., 2001b). These granites have high alkali contents ($Na_2O+ K_2O=6.1\%$) and K_2O (K_2O/Na_2O ratio of 1.2–2.3), and show characteristics of A-type granites. Strong depletion in MREE and a negative Eu anomaly suggest strong fractional crystallization of the granitic magma. Strong positive anomalies for HFSE (Zr, Hf, Nb, Ta, Th) and LILE (Rb, K, Ba) also suggest an A-type granite affinity. The initial $^{87}Sr/^{86}Sr$ ratios for these granites range from 0.7044 to 0.7095 (Hou et al., 2001b), implying a mantle or crust/mantle mixed source for the A-type granite magma.

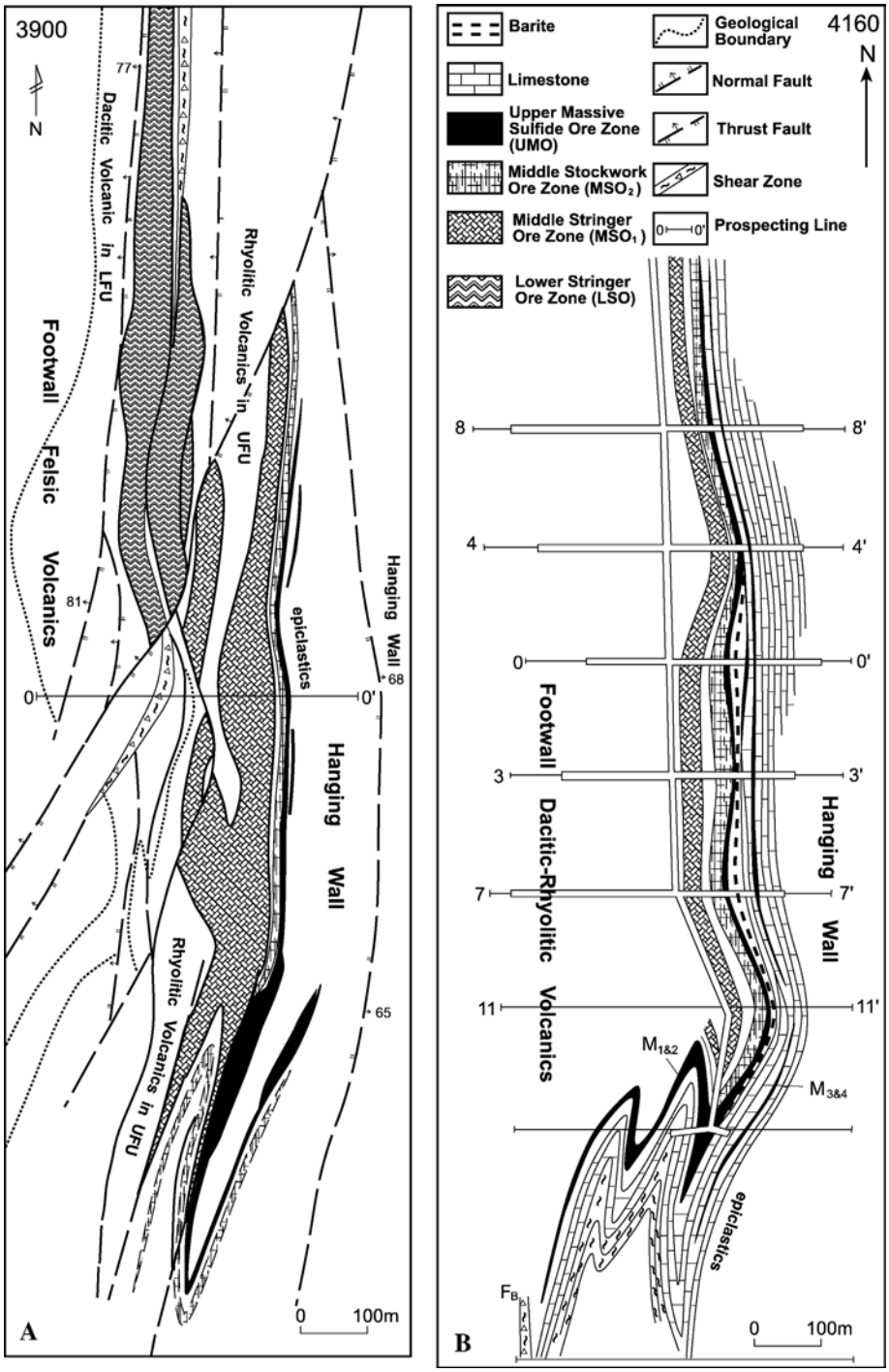

Fig. 12. Plan maps at 3190 m (A) and 4160 m (B) showing vertical variation in geometry and shape of the orebodies at the Gacun deposit (modified from Xu et al., 1993).

Based on the host rock type and mineralization characteristics, at least two ore types have been recognized: (1) skarn-type Sn (–Ag) deposit occurring along the contact between an A-type granite and Upper Triassic limestone; and (2) vein-type Ag (-polymetallic) deposit hosted in an Upper Triassic slate sequence surrounding the A-type granite intrusions. The skarn-type deposits include the medium-sized Lianlong Sn

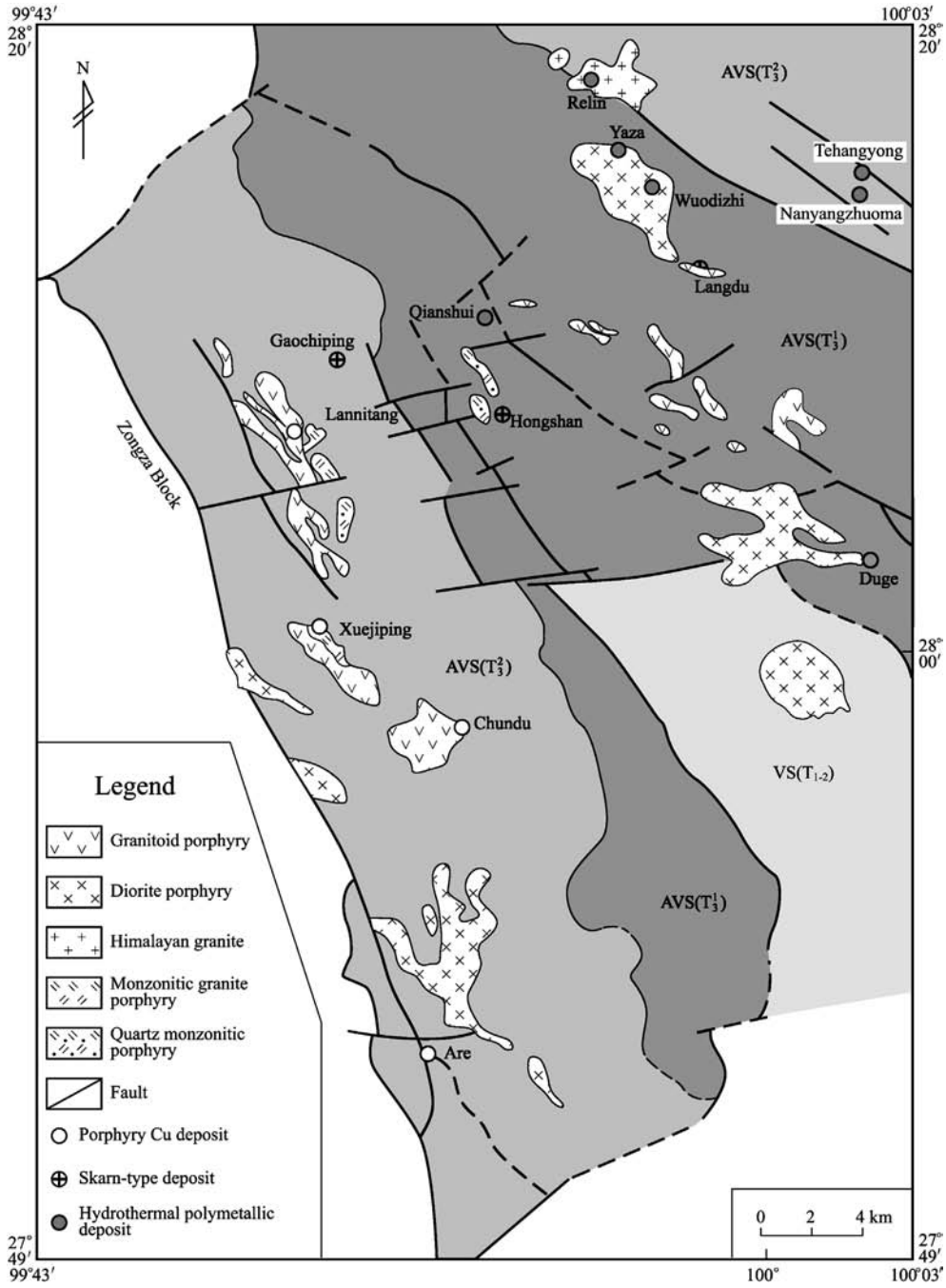

Fig. 13. Sketch map showing the volcano-intrusion complex and related mineralization in the Zhongdian arc, southern segment of the Yidun island-arc. AVS (T_3^1): Late-Triassic arc volcanic–sedimentary sequence (Lower); AVS (T_3^2): Late-Triassic arc volcanic–sedimentary sequence (Upper); VS (T_{1-2}): Early–Middle Triassic volcanic–sedimentary sequence.

deposit and numerous small deposits along the inner and outer contacts of the A-type granite belt. The vein-type deposits include the large Xiasai Ag deposit and other smaller deposits controlled by a NNW-striking fault system in the periphery (1–10 km) of the granite intrusions (Fig. 10).

In the Lianlong district, the skarn-type Sn–Ag deposits mainly occur in diopside skarn at the outer contact zone, and in grossular skarn at the inner contact zone. Minor orebodies are hosted in the vesuvianite skarn and melilite skarn that formed from replacement of argillaceous rocks. Ore minerals include cassiterite,

stannite, native bismuth, arsenopyrite, pyrite, galena, sphalerite and scheelite. The $\delta^{34}S$ value of a granite sample is usually light, −8.1‰, and the $\delta^{34}S$ values of eight sulphide samples are also unusually light, from −9.5 to −10.5 (Qu et al., 2001). The $\delta^{34}S$-enrichment order for the sulphide minerals shows that the S isotope equilibrium was not reached during the deposition of the sulphides. The coincidence in $\delta^{34}S$ values of sulphides with host granites suggests that the ore sulphur was primarily derived from granite magma. The Pb isotopic compositions of sulphide ores and host granites vary in the transitional range for $^{207}Pb/^{204}Pb$ and $^{206}Pb/^{204}Pb$ ratios between the orogenic belt and the upper crust (Qu et al., 2001), suggesting an upper crust source beneath the Yidun arc.

In the Xiasai district, sulphide orebodies mainly occur as stratabound, lenticular or stringer assemblages in the interlayered *decollement* zones between the Upper Triassic sandstone–siltstone and sericitic slate. These orebodies are controlled by a NNW-striking fault system. Intense linear hydrothermal alteration was well-developed along the fault system, and shows a horizontal zoning of silicification–sericitization–carbonation–chloritization–actinolitization from the center of the orebody to the wall rocks. The fault system appears to have served not only as a passageway for hydrothermal fluids, but also as a major ore-hosting space. Silver-rich Zn ore and Ag–Zn–Pb–Cu–Sn ores are the dominant ore types, and normally have massive, brecciated, banded and mottled structures. The major ore minerals include metallic sulphides, Ag-bearing sulphide minerals (Cu–Sb–Ag and Sb–Ag) and Bi- and Sb-bearing lead sulphides (Pb–Sb and Pb–Bi). Sulphur isotopic analysis of 15 sulphide samples yields a range of $\delta^{34}S$ values from −4.9 to −10.5‰ (aver. −8.2‰). The Pb isotope analyses of 15 ore samples show that $^{207}Pb/^{204}Pb$ ratios vary between 15.095 and 15.902, $^{206}Pb/^{204}Pb$ ratios between 18.687 and 18.874 and $^{208}Pb/^{204}Pb$ ratios between 38.962 and 39.737, suggesting more radiogenic Pb for the ore. In the $^{207}Pb/^{204}Pb$ versus $^{206}Pb/^{204}Pb$ diagram, the sulphide Pb yields a linear array across the upper crustal growth line. This indicates that ore-forming hydrothermal fluids leached most of the Pb ore from strata in the upper crust.

3.6. Jinshajiang VHMS polymetallic belt

This is one of the most significant polymetallic belts in the STMD. The belt is 60 km wide and more than 500 km long, extending from Eastern Tibet, Western Yunnan to Western Sichuan (Fig. 14). It is tectonically located in the Jinshajiang tectono-magmatic belt, and includes a collage of the Changdu continental block joined by Palaeozoic Jinshajiang ophiolitic sutures and the Permian Jamda–Weixi volcano-plutonic arc (see Fig. 2; Mo et al., 1993; Liu et al., 1993; Hou et al., 1999).

Four secondary tectonic units have been recognized: the foreland fold–thrust zone, ophiolite mélange zone, superimposed rift zone and continent-marginal volcanic arc zone, from east to west across the belt (Fig. 14; Wang et al., 1999a,b). The foreland fold–thrust zone comprises Early Palaeozoic carbonate, turbidites, mafic lavas and volcaniclastic rocks, which were thrusted eastward as a structural slab or folded zone during arc–continent collision. The ophiolitic mélange zone is 20–40 km wide and over 1000 km long, and is unconformably overlain by the Late Triassic red beds. The ophiolitic suite in the zone comprises lower mafic–ultramafic rocks, mid-ocean ridge basalt (MORB) and ocean–island basalt (OIB), diabase dikes, plagiogranites and radiolarian siliceous rocks (Mo et al., 1993; Hou et al., 1996a,b). The mafic lavas yield U–Pb zircon ages varying from 361.6 Ma to 269.1 Ma (Zhan et al., 1998); the plagiogranites also have a similar U–Pb age range from 340±3 Ma to 294±3 Ma (Wang et al., 1999b).

The intra-oceanic arc volcanic sequence, consisting of tholeiitic lava and calc-alkaline andesites, overlies the ophiolitic mélange zone and yields a Rb–Sr isochron age range of 268.7–257.1 Ma (Wang et al., 1999a). The continental margin arc zone is dominated by a Permian arc volcano-sedimentary sequence at the eastern margin of the Changdu continental block (Figs. 2 and 14). Tholeiitic, calc-alkaline and shoshonitic volcanic and intrusive rocks were emplaced successively on the continental margin arc. The extensional rift basin zone is superimposed on the Permian Jamda–Weixi arc (Fig. 14). The lower part of the rift basin was filled by Late-Triassic bimodal volcanic rocks and deep-water flysch sediments. The upper part was filled by shallow-water intermediate to felsic volcanic rocks and limestone (Wang et al., 2003b).

The VHMS deposits in the polymetallic belt mainly occur in Permian intra-oceanic arc volcanic rocks and in the Late Triassic volcanic district (Fig. 14). In the Permian marine volcanic district, VHMS deposits occur in a calc-alkaline volcanic sequence that was overlain by siliceous phyllic slate and sandstone. The Yagra Cu deposit is typical, comprising an upper stratiform massive sulphide ore zone and an underlying stringer–stockwork ore zone (Fig. 15). The massive sulphide orebodies occur in or near stratabound beds (Zhan et al., 1998), and are conformably overlain by abyssal black shale, whereas the stringer–

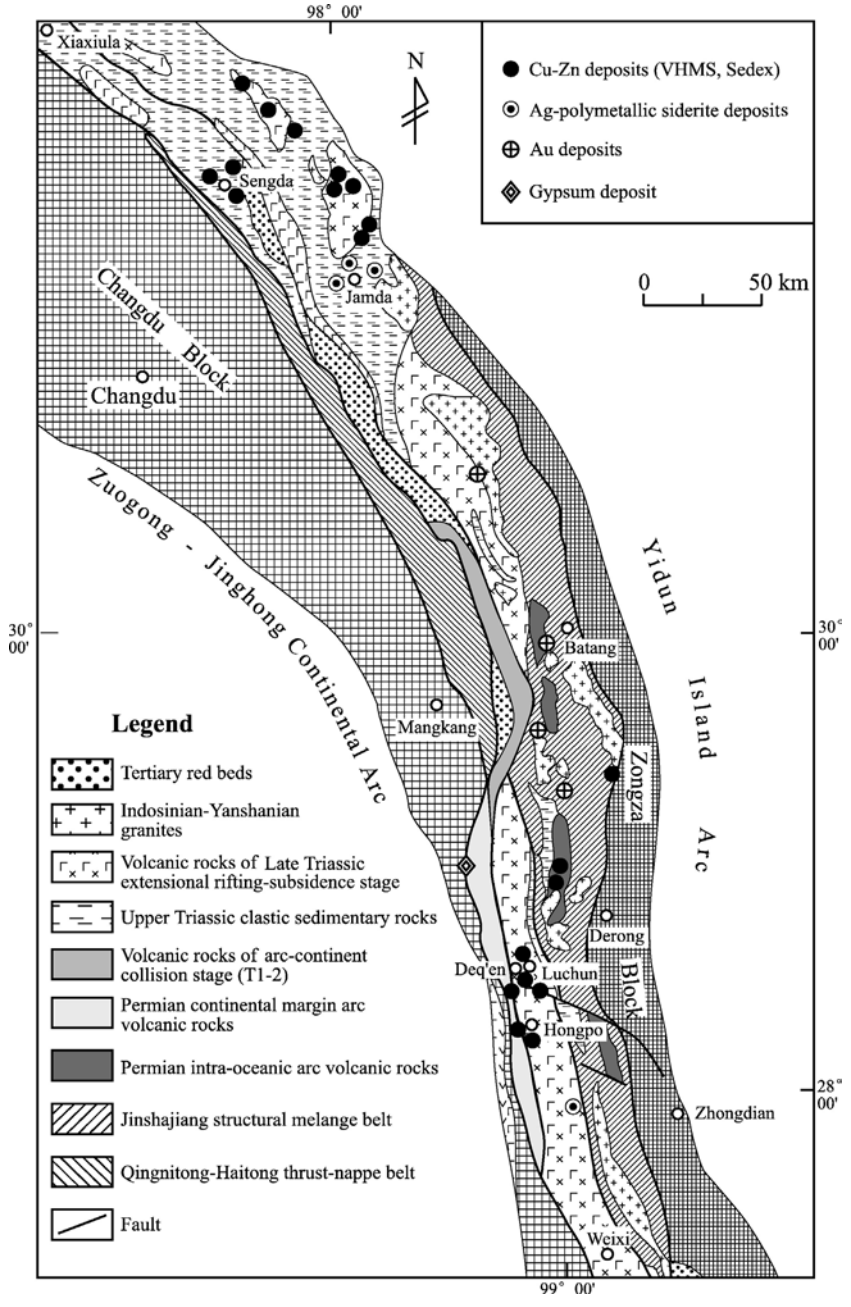

Fig. 14. Sketch geological map showing the tectonic framework and the distribution of volcanic rocks of the Jinshajiang polymetallic belt (after Hou et al., 2003b).

stockwork ore zone is hosted in the calc-alkaline andesitic volcanic rocks. Active hydrothermal system and base-metal deposits have been observed in similar environments on the modern seafloor (Rona, 1984; Rona and Scott, 1993). A typical example is from a forearc caldera developed along the Isuzu arc, in which a Kuroko-type deposit, with ore reserves occupying 80% of the total ore reserves of the 432 known Kuroko deposits in the world, was discovered recently (Iizasa et al., 1999).

In the Late Triassic bimodal volcanic district, VHMS deposits are associated with marine felsic-volcanic complexes and cluster in Late Triassic rift basins. These deposits are stratiform to stratabound and, in most

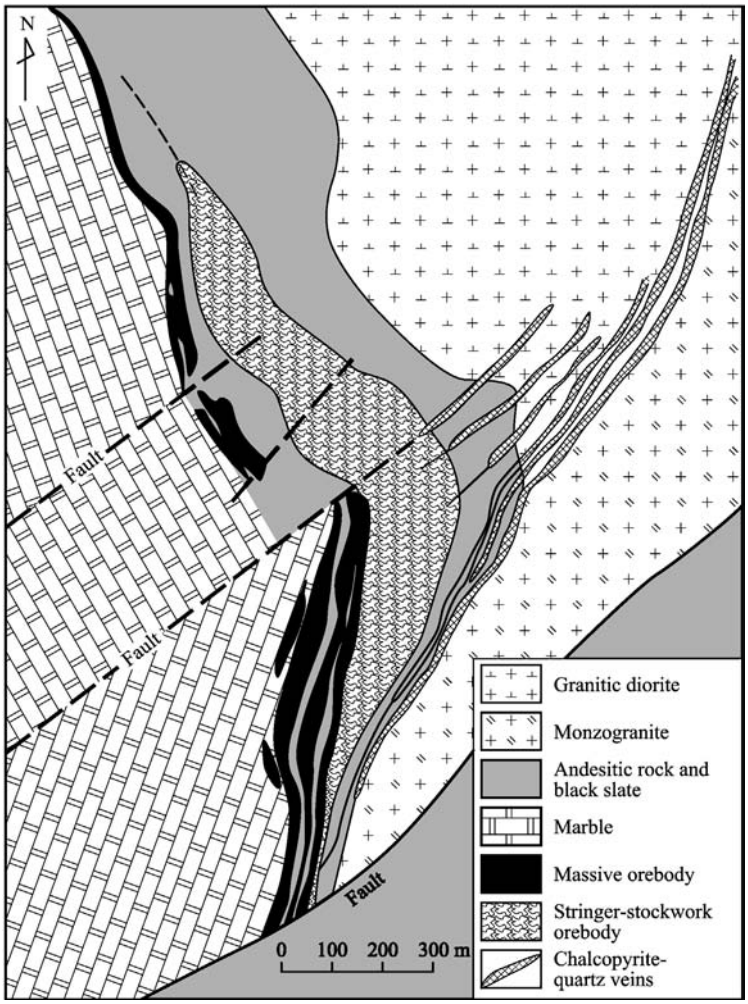

Fig. 15. Simplified geological map of the Yagra Cu deposit in the Jinshajiang polymetallic belt, SW China (after Hou et al., 2003b).

cases, are closely associated with chert and banded dolomite. The Luchun deposit is a typical deposit in the district. In addition, a number of smaller deposits, occurrences and mineralized prospects have been discovered in the district (Fig. 14). The Luchun deposit occurs in the Xuzhong–Luchun basin within the Late Triassic rifting zone, in which alternating basalts and rhyolites were developed. Sulphide orebodies are hosted in the calc-alkaline felsic volcanic rocks with Rb–Sr isochron ages ranging between 224 Ma and 239 Ma, and are conformably overlain by laminar siliceous rocks and banded limestone, turbidite and fine clastic rocks. The deposit is composed of the lower stringer–stockwork ore zone and an overlying stratiform–stratabound massive sulphide zone. The massive sulphide orebodies are normally associated with sulphide-bearing chert, black pyritic shale and banded limestone, and display laminated and banded structures and graded bedding. The lower stringer–stockwork orebody is characterized by a well-developed alteration pipe with distinct zonation from the silicification zone through the sericitization zone to the sericitization–chloritization zone outwards. Six sulphide samples from the deposit yield $\delta^{34}S$ values of 12.6‰–14.7‰ (Li et al., 2000), suggesting a seawater sulphate source for ore S. Their Pb isotope compositions are $^{207}Pb/^{204}Pb = 15.5879–15.6571$, $^{206}Pb/^{204}Pb = 18.4981–18.5435$ and $^{208}Pb/^{204}Pb = 38.4298–38.6480$ (Li et al., 2000), among which the $^{207}Pb/^{204}Pb$ ratio is close to that of the crustal Pb. This shows that the major source of the Pb ore was probably the volcano-sedimentary arc sequence.

In the Late Triassic intermediate to felsic volcanic district, VHMS deposits are mainly hosted in calc-

alkaline dacitic–rhyolitic volcanic rocks and the contact zones between the overlying thick-bedded micrite and medium- to thin-bedded grayish-green sandstone (Fig. 14). The disseminated, veined and lenticular orebodies occur within the stratiform to stratabound siderite beds, and are closely associated with barite-rich cherts. The VHMS deposits in the district include the Zhaokalong and Dingqennong Fe–Ag-polymetallic deposits and the Chugezha Fe–Ag siderite deposit. The following four lines of evidence indicate that these VHMS deposits formed in a shallow-water volcanic environment: (1) the host rocks are mainly pyroclastic volcanic rocks with ignimbritic texture and purplish dark grey-red colour at the top (Wang et al., 2000b), and conformably overlie the Upper Triassic purplish-red subaerial molasse clastic rocks; (2) the siderite bed, as a host rock for sulphide orebodies, comprises a significant ore-equivalent horizon closely associated with massive sulphide orebodies, suggesting a strong oxidizing environment during hydrothermal activity and sulphide mineralization; (3) massive dolomite on the top, or at the edges, of massive sulphide orebodies at Zhaokalong and Dingqinlong occur in many shallow-water VHMS deposits (Carvalho, 1991; Galley et al., 1993; Halley and Roberts, 1997); and (4) the strong silicification of the footwall rocks is typical of shallow-water VHMS deposits (Halley and Roberts, 1997). Extensive fluid boiling commonly occurred in the shallow-water environments as a result of rapid precipitation of large amounts of SiO_2 and sulphides in the sub-seafloor to form strongly silicified rocks and stockwork-disseminated ores (Lydon, 1988; Large, 1992).

4. Major metallogenic epochs

Metallogenesis in the STMD, accompanying the tectonic evolution of the Sanjiang Tethys from the Palaeozoic arc-basin system through Mesozoic collisional Orogeny to Cenozoic intra-continental convergence, can be divided into four epochs: the Early Palaeozoic, Late Palaeozoic, Late Triassic and Himalayan metallogenic epochs, based on ore-bearing formation characteristics and direct or indirect mineralization ages (Fig. 16). Metallogenic processes mainly occurred in the last two epochs.

4.1. Early Palaeozoic metallogenic epoch

The metallogenic processes during this epoch mainly developed along the margins of continental blocks (e.g., Zongza and Baoshan blocks) in the Sanjiang Tethys, and formed exhalative-sedimentary Pb–Zn deposits hosted in Early Palaeozoic marine carbonate rocks (e.g., Luzijuan and Najiaoxi Pb–Zn deposits). This metallogenic epoch occurred mainly in the Cambrian–Ordovician periods, spanned an isotopic age range of 426–655 Ma for mineralization (Liu et al., 1993) and is characterized by medium-sized and limited Pb–Zn mineralization (Fig. 2).

4.2. Late Palaeozoic metallogenic epoch

This metallogenic epoch is mainly represented in marine volcanic environments, arc or back-arc basins, and is characterized by the formation of VHMS

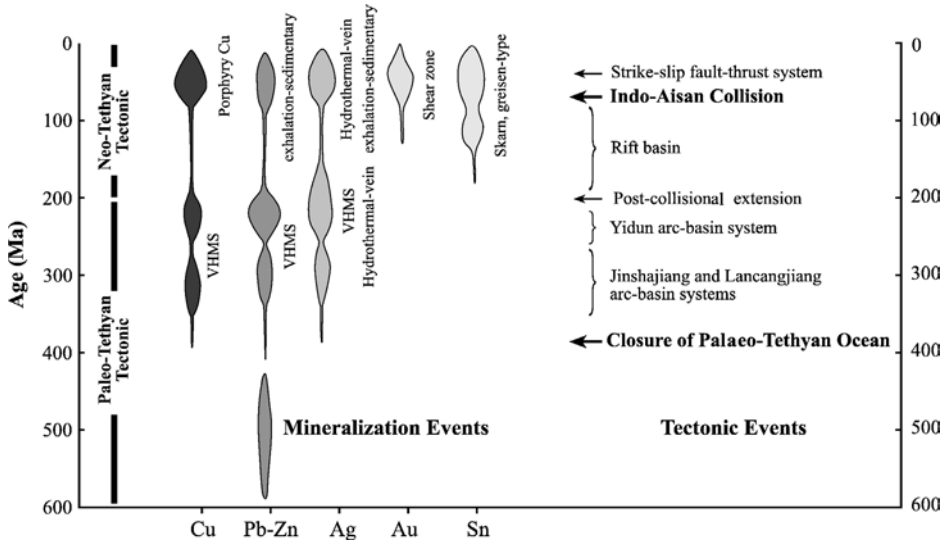

Fig. 16. Sketch illustrating the main metallogenic epoch and its relationship with main tectonic events in the STMD.

deposits. In the Changning–Menglian back-arc basin (Fig. 2), the Laochang Pb–Zn–Ag deposit occurs in the Carboniferous alkaline intermediate–mafic volcanic district, whereas the Tongchangjie Cu deposit is hosted in Permian basaltic volcanic rocks with MORB affinity (Yang et al., 1992). In the intra-oceanic arc related to the Jinshajiang slab subduction, the Yagra-style Cu deposits were developed in Permian calc-alkaline andesitic rocks, whereas in the volcanic arc related to Lancangjiang slab subduction, the Sandashan-style Cu deposit occurs in the Late Permian marine calc-alkaline dacitic–rhyolitic volcanic rocks. In general, this metallogenic epoch is characterized by Cu mineralization with minor Zn and Pb, and was a significant period for the formation of massive sulphide Cu deposits in the STMD.

4.3. Late Triassic metallogenic epoch

The Late Triassic metallogenic epoch is one of the most important metallogenic epochs due to the large number of polymetallic deposits that developed in some rift basins or extensional basins in STMD. In the Late Triassic Yidun island-arc, the Gacun-style VHMS deposits cluster in the intra-arc rift basins (Fig. 10), and are hosted by Triassic marine calc-alkaline rhyolitic piles associated with basalts (Hou et al., 1995, 2001a). Rhenium–Os isotope dating of sulphide ores yields a mineralization age of 217 Ma for the Gacun VHMS deposit (Hou et al., 2003c). The Late Triassic extensional basin developed on the Permian Jamda–Weixi arc. The Luchun-style VHMS deposits occurred in a marine bimodal rhyolitic–basaltic volcanic district (Fig. 14). The Rb–Sr isochron age for the host rhyolites (235 ±7 Ma; Wang et al., 2002) constrains a Late Triassic mineralization age for the Luchun deposit. The Zhaokalong-style VHMS Ag-polymetallic deposits occurred in a shallow-water intermediate–felsic volcanic environment within the extensional basins. Regional stratigraphic correlation and fossil evidence constrain the mineralization to the end of the Triassic. In the Late Triassic rift basins that developed inside the Changdu–Simao continental block, a large number of exhalative-sedimentary deposits, such as the Huishan and Yanzidong Ag–Cu–Pb–Zn deposits, the Xiawuqu Ag deposit and the Dongzhiyan Sr deposit, were hosted in a sedimentary sequence in Upper Triassic Sanhedong Formation (Fig. 8). The Sanhedong Formation is composed of siliceous rock, laminar fine-crystalline dolomite and dolomitic limestone (Wang et al., 2000a).

In general, it appears that the mineralization formed in a relatively short time but the extent of mineralization was much larger in this metallogenic epoch than those of the other epochs. The development of precious metal Ag-rich massive-sulphide deposits and large amounts of sulphate accumulations (barite, siderite, gypsum and celestite) characterize metallogenesis in this epoch.

4.4. Himalayan metallogenic epoch

This is the most important metallogenic epoch in the STMD. The ore deposits formed during this period account for 70% of the total of the STMD. The metallogeny is closely related to the large-scale strike-slip fault system, nappe-thrust system and tectonic–magmatic belts in the Sanjiang Tethys, which were caused by the Indo-Asian collision since the Palaeocene. Many giant deposits were formed in this epoch, including the Yulong porphyry Cu deposit (Fig. 6), Jinding Pb–Zn deposit (Fig. 9), Ailaoshan Au deposit (Figs. 3 and 4), Lailishan Sn deposit and Baihuanao rare metallic deposit (Fig. 7). The geochronological data for the Yulong ore-bearing porphyry belt, controlled by a right-lateral strike-slip fault system, give a shallow-level emplacement age range of 33–52 Ma (Ma, 1990). Rhenium–Os isotopes for molydenites from these porphyry copper deposits yielded an age of 36 to 40 Ma for copper mineralization (Du et al., 1994; Hou et al., 2006). The K–Ar ages of 51.1–59.8 Ma for the Lailishan and Baihuanao K-feldspar granite units constrain the Himalayan epoch and mineralization age for the Lailishan Sn deposit and Baihuanao rare metal deposit in the Chayu–Tengchong granite belt.

The Ailaoshan-style Au deposits that occur in the ophiolitic mélange zone have been affected by strong napping and shearing. Although these deposits have a wide mineralization age range varying from 96 Ma to 28 Ma, they mostly formed during the Himalayan epoch (Liu et al., 1993; Hu et al., 1995; Huang et al., 1997). Similar Au deposits occur in the Garze–Litang ophiolitic mélange belt, and they are also most likely to have developed during the Himalayan epoch (Zhang et al., 1998b).

In the Simao continental block, the development of a series of strike-slip pull-apart basins and nappe-detachment zones, controlled by a Tertiary strike-slip fault system (Liu et al., 1993), led to a number of hydrothermal vein-type Ag–Cu-polymetallic deposits (e.g., Baiyangping and Fulongchang), exhalative-sedimentary Ag–Pb–Zn deposits (e.g., Huishan, Yanzidong and Xiawuqu), exhalative-replacement Pb–Zn deposits (e.g., Jinding) and sedimentary–hydrothermal overprinted Cu–Ag-polymetallic deposits (e.g., Baiyangchang). In the Yidun island-arc, the emplacement of the

Yanshanian A-type granite belt, as a marked product of orogenic collapse, led not only to the formation of skarn-type or vein-type Sn-polymetallic deposits, and but also to development of hydrothermal vein-type Ag deposits (e.g., Xiasai).

In summary, extensive mineralization, large deposits, complex metallic associations and a large variety of metallogenic ore types characterize the Himalayan metallogenesis as the most economically significant epoch in the STMD.

5. Tectonic setting and metallogenic environments

Metallogenesis in the STMD primarily occurred in the three significant tectonic settings. They are: (1) a trench–arc–basin system related to slab subduction, in which submarine hydrothermal and epithermal ore-forming processes were mainly developed; (2) a post-collision crustal extensional setting, where mainly deep-water and/or shallow-water submarine hydrothermal mineralization process occurred in extensional or rift basins; and (3) NW-trending large-scale strike-slip and thrust–nappe systems caused by the Indo-Asian continent collision since the Palaeocene, in which porphyry Cu deposits, skarn deposits, granite-related Sn and rare metal deposits, hydrothermal vein-type Ag polymetallic deposits, and shear zone-type Au deposits were developed.

5.1. Arc-basin system related to subduction

Three arc-basin systems have been recognized in the Sanjiang Tethys, i.e., the Yidun island-arc, the Jamda–Weixi continental margin arc and the Zuogong–Jinghong continental margin arc (Mo et al., 1993). Despite having different tectonic histories, they all show significant potential for base metal mineralization.

The Triassic Yidun island-arc, as the product of westward subduction of the Garze–Litang oceanic slab, preserves a well-developed trench–arc–basin system, though arc–continent collision and crustal shortening has occurred since the Early Jurassic (Hou, 1993; Hou et al., 1995, 2001a). Four tectonic units have been recognized across the island-arc from east to west: the Garze–Litang trench, Daocheng forearc, Zengke–Zhongdian volcano-magmatic arc, and Miange back-arc basin. There are certain differences in stress situations, volcanic successions and associated mineralization along this arc. The Zhongdian arc, the southern segment of the arc system, is characterized by calc-alkaline andesitic–dacitic volcanic rocks and associated porphyry complexes with porphyry Cu deposits and skarn-type Cu polymetallic deposits, together with an inactive back-arc spreading basin (Ye et al., 1992; Hou et al., 1995). The Changtai arc, the northern segment of the arc system, is characterized by the development of the intra-arc rifting zone that splits along the volcanic arc and the back-arc basin (Hou and Mo, 1993; Hou, 1993). The intra-arc rift zone, marked by a bimodal basaltic–rhyolitic suite, with a Rb–Sr isochron age of 217 Ma, and deep abyssal marine basins, constrains the temporal–spatial localization of the submarine hydrothermal system and the Gacun-style VHMS deposits (Hou, 1993; Hou et al., 2001a). The Miange back-arc basin is characterized by a bimodal shoshonite–high-K rhyolite association, with a Rb–Sr isochron age of 213 Ma (Hu et al., 1992), and a black shale sequence. The epithermal Ag–Au–Hg deposits occur in the high-K rhyolitic volcanic rocks.

The Permian Jamda–Weixi continental margin arc, imposed on the Early Permian Chubrong–Dongzhulin intra-oceanic arc (Fig. 17), is a product of westward subduction of the Jinshajiang–Ailaoshan oceanic slab, marked by Carboniferous–Permian ophiolite mélange (Wang et al., 1999a,b) and abyssal arenaceous flysch formations (Liu et al., 1993). The Jinshajiang–Ailaoshan ophiolitic mélange complex hosts the Ailaoshan-style lode Au deposit, which is an important ore-forming metal and ore type in the belt (Hu et al., 1995). The Chubrong–Dongzhulin intra-oceanic arc is mainly composed of basal tholeiitic basalts and overlying calc-alkaline andesitic–dacitic volcanic rocks with Rb–Sr isochron ages of 268.7–257.1 Ma (Wang et al., 1999a). A mixed sequence of arc volcanic rocks with overlying phyllic slate–sandstone host the Yagra-style VHMS Cu deposits (Fig. 17). Although the Late Permian Jamda–Weixi continental margin arc along the eastern edge of the Changdu–Simao block is similar to the Andean arc (Mo et al., 1993), Cordilleran-type porphyry Cu deposits have not been recorded because of lack of the granitic (felsic) porphyries.

The Zuogong–Jinghong continental arc, tectonically similar to the Jamda–Weixi arc, was caused by subduction of the Lancangjiang oceanic slab beneath the Changdu–Simao block in the Early Permian (Mo et al., 1993). At present, only some small polymetallic occurrences have been discovered in the volcanic arc, and its economic potential needs to be evaluated further.

5.2. Post-collisional crustal extension

Collisional orogeny, initiated with the subduction of continental crust, usually involves complex processes such as crustal shortening and thickening, mountain-

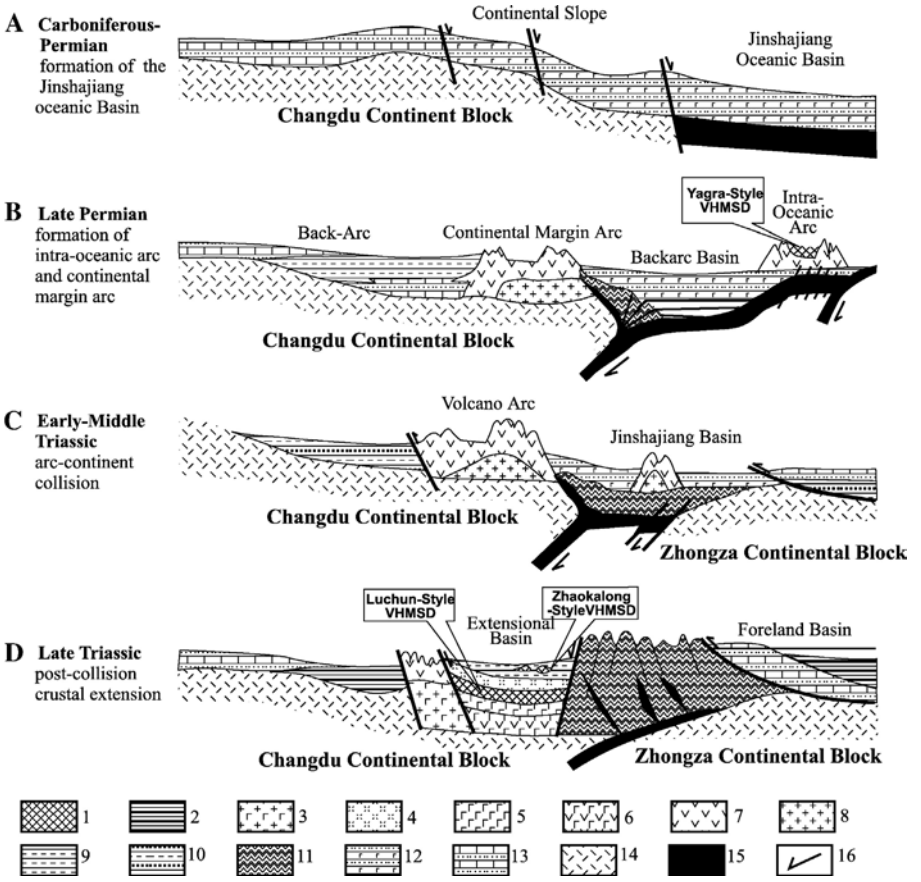

Fig. 17. Schematic of tectonic evolution and ore-forming environments of VHMS deposits in the Jinshajiang polymetallic belt (after Wang et al., 1999a,b; Hou et al., 2003b). 1. orebody or deposit; 2. abyssal flysch; 3. bimodal volcanic rocks; 4. rhyolite; 5. basalt; 6. intermediate–mafic arc volcanic rocks; 7. intermediate–felsic arc volcanic rocks; 8. granitic intrusive rocks; 9. marginal clastic rocks; 10. platform clastic rocks; 11. structural melange; 12. basin volcanic rocks; 13. platform carbonate rocks; 14. crustal basement; 15. oceanic crust; 16. subduction direction.

root delamination, post-collisional extension and mountain collapse (Dewey, 1988). In the Sanjiang region, the collisional orogenic process occurred on both sides of the Changdu–Simao block. The area entered into a lithospheric extension stage during the Early Triassic and then into arc–continent collision with crustal shortening and thickening in the Late Triassic. The post-collisional crustal extension is indicative of the changes from intensive compression to regional extension, from an arc volcanic association to a bimodal suite, and from collision–uplift to rift–subsidence. This event resulted in large-scale and extensive mineralization processes in the Late Triassic.

The arc–continent collision along the eastern margin of the Changdu–Simao block in the Early–Middle Triassic resulted in a limited distribution of high-Si and -Al rhyolitic volcanic rocks imposed on the Jamda–Weixi arc (Mo et al., 1993). Post-collision intensive extension led to the Late Triassic basalt–rhyolite bimodal volcanism, with a Rb–Sr isochron age range of 235–239 Ma (Wang et al., 2002), bringing about rifting or development of fault-bounded basins along the continental marginal arc (Figs. 14 and 17; Wang et al., 1999a). At least three ore-bearing rift basins have been identified from the north to the south: the Sinda–Chesuo basin, Xuzhong–Luchun basin, and Reshuitang–Cuiyibi basin. The filling sequence of the basins is as follows: bathyal basaltic volcanic rocks–diabase complex and flysch sedimentary rocks in the lower part, abyssal interbedded basalt–rhyolite bimodal suite and argillaceous rocks in the middle part, shallow-sea rhyolitic volcanic rocks and sandy mudstone in the upper part, and littoral–neritic molasse clastic rocks and overlying intermediate–felsic pyroclastic rocks associated with gypsum formation at the top.

The aforementioned Late-Triassic volcano-sedimentary sequence records a history of this basin development by intensive pull-apart and rifting processes in the

Early–Middle stage, to gradual shrinking and dying in the late stage. The Luchun-style VHMS deposits and Chugezha-style VHMS deposits occur in the Xuzhong–Luchun basin (Fig. 17). The former were developed in the pull-apart stage and are hosted in the bimodal rhyolitic volcanic complex in the lower part of the basin (Wang et al., 1999a). The latter formed in the closure stage and are hosted in felsic pyroclastic rocks in the upper part of the basin, where siderite beds occur persistently as host rocks and are parallel to the wallrock strata. The Zuna-style exhalative-sedimentary deposits and the Zhaokalong-style VHMS deposits were developed in the Sunda–Chesuo basin. The former occur as stratiform and banded orebodies in abyssal sandy–muddy rocks at the bottom of the basin. The latter is hosted in a shallow-water felsic pyroclastic succession in the upper part of the basin, and occurs as disseminated, stringer and stockwork orebodies strictly confined by the stratified siderite beds (Liu et al., 1993). Similar shallow-water VHMS deposits have been widely reported (Carvalho, 1991; Galley et al., 1993; Halley and Roberts, 1997).

The post-collisional extension event along the western margin of the Changdu–Simao block also took place in the Late Triassic, and the marker product is the potassic trachybasalt–rhyolite bimodal suite of the Upper Triassic Manghuihe Formation (Mo et al., 1993), accompanied by VHMS mineralization. The Wenyu Cu deposit of Jingdong County is hosted in a high-K trachybasalt and the Minle Cu deposit of Jinggu County is hosted in a high-K rhyolite pile, indicating the constraints of the post-collisional crustal extension and the submarine hydrothermal mineralization system. A similar post-collisional crustal extension setting, as a significant environment for VHMS deposits in the Mt. Read volcanic belt (MRV) in western Tasmania, Australia, has been suggested (Crawford et al., 1992; Crawford and Berry, 1992).

In the central part of the Changdu–Simao block a rifting event formed intra-continental rift basins in the Late Triassic, such as the Lanping basin, and was accompanied by extensive hydrothermal mineralization processes. The venting and discharging of fluids from the hydrothermal system through syn-faulting zones resulted in the formation of large amounts of hydrothermal cherts and polymetallic deposits hosted in the Upper Triassic Sanhedong Formation (Fig. 8). These exhalative-sedimentary deposits suffered from hydrothermal overprinting in the Himalayan epoch but still preserve primary characteristics of exhalative deposition.

There are two possible mechanisms to explain the post-collisional crustal extension at the Late Triassic. One is the lithospheric delamination that probably occurred beneath the Changdu–Simao continental block. The delamination would have directly caused the rise of hot asthenosphere to reach the crust–mantle boundary and replace the cool lithosphere; thinned and heated lithosphere was rapidly raised and subsequent extension took place (Bird, 1979; Sacks and Secor, 1990). As a result of depressurization and partial melting due to the asthenospheric uplift, basaltic magma was intruded into the lower crust and the heated crust would have enhanced the melting to form felsic magma emplaced upwards into the upper crust (Powell, 1986). Therefore, large-scale underplating of basaltic magma and eruption of shoshonitic magma are usually regarded as petrographic evidence for lithospheric delamination (Kay, 1994; Kay and Kay, 1994; Dong, 1999). Another model is the breaking-off of subducted slab (e.g., Jinshajiang and Lancangjiang slabs), which is interpreted to have been caused jointly by the buoyancy of the subducted continental crust and the downward dragging force of the subducted oceanic crust. Slab break-off would have led directly to large-scale upwelling of the asthenosphere and partial melting of the lower crust, so that subsequently extensive felsic magmatism produced abundant syn-collisional granitoids (Davies and Blanckenburg, 1995). The global seismic–tomographic images demonstrate that the Tethyan subducting slab materials were extensively broken and subsided back to the mantle to a depth of about 1200 km (Fukao et al., 1994). The seismic–tomographic images over the Sanjiang area also show that the subducting slab was broken off and returned to the mantle (Zhong et al., 2001). The bimodal volcanism, shoshonitic volcanic rocks and rift basins in the Changdu–Simao block manifest that lithospheric delamination or subducting slab break-off indeed began in the Late Triassic.

The upwelling of the asthenosphere in the Sanjiang Tethys not only resulted in mantle-derived and crust-derived magmatism, but also provided large quantities of ore-forming materials. The intensive crustal extension and large thermal anomalies induced by the hot mantle upwelling might have led to large-scale convection and circulation and long-distance migration of the fluids along pull-apart fractures. These are probably the major geodynamic and tectonic processes for metallogenesis in the Late Triassic.

5.3. Large-scale strike-slip faulting and thrusting systems

Collision of the Indian–Asian continent, initiated during the Palaeocene, led to the formation of the

Himalayan Orogen, which caused intense shortening and double thickening of the crust in the interior Plateau, as well as the formation of the extensive syn-collisional Gangdese granitoid belt at ca. 55 Ma (Allegre et al., 1984). Coincident continent–continent collision caused right-lateral shearing along the eastern margin of the converging continents, resulting in the formation of large-scale strike-slip faulting and thrust systems in East Tibet (Tapponnier and Molnar, 1976; Peltzer and Tapponnier, 1988; England and Molnar, 1990; Yin and Harrison, 2000), which in turn controlled the formation and distribution of the large-scale and giant Himalayan deposits in the Sanjiang Tethys.

5.3.1. Strike-slip fault system

The Sanjiang strike-slip fault system, which trends roughly orthogonal to the orientation of convergence between Asia and India during the Palaeocene–Eocene boundary, was composed of a series of small right-lateral strike-slip faults, such as the Chesuo Fault, Wenquan Fault and Tuoba Fault (Figs. 1 and 5). These faults are intersected by a series of NW–NNW-trending sinistral *en echelon* folds and compressional sinistral faults, and these intersections appear to have controlled the localization of ore-bearing porphyries (Fig. 5). Relaxation of regional stress and transition of strike-slip movement and direction occurred in the east of the Himalayan orogen, accompanying the Asia–India collision, but the exact timing of the transition is not well constrained. The stress relaxation is probably related to north-eastward wedging of the Indian continent and its collision with the Yangtze continent during the Palaeocene–Eocene, which caused intense E–W compression, and the conjugate strike-slip movement in the Sanjiang Tethys, which resulted in the formation of an 'X'-shaped structural knot with Deqen as the center (Fig. 18).

The Simao block at the southern end of the structural knot slipped southwards extensively along the Honghe sinistral strike-slip fault at about 23 Ma (Tapponnier et al., 1990), and resulted in a series of strike-slip pull-apart basins, such as the Lanping–Yunlong basin and the Jiangcheng–Mengla basin. These basins are filled up with thick continental salt-bearing formations, with the upper part having slump accumulations of fluviolacustrine fan sedimentary rocks. The Changdu block was displaced northward along the strike-slip faults and formed a group of strike-slip extensional basins, such as the Gonjo and Nangqen pull-apart basins. These basins contain more than 2600 m-thick Tertiary red bed sedimentary rocks interlayered with latitic–trachytic volcanic rocks with a $^{40}Ar/^{39}Ar$ age range of 36–42 Ma (Zhang and Xie, 1997; Chung et al., 1998).

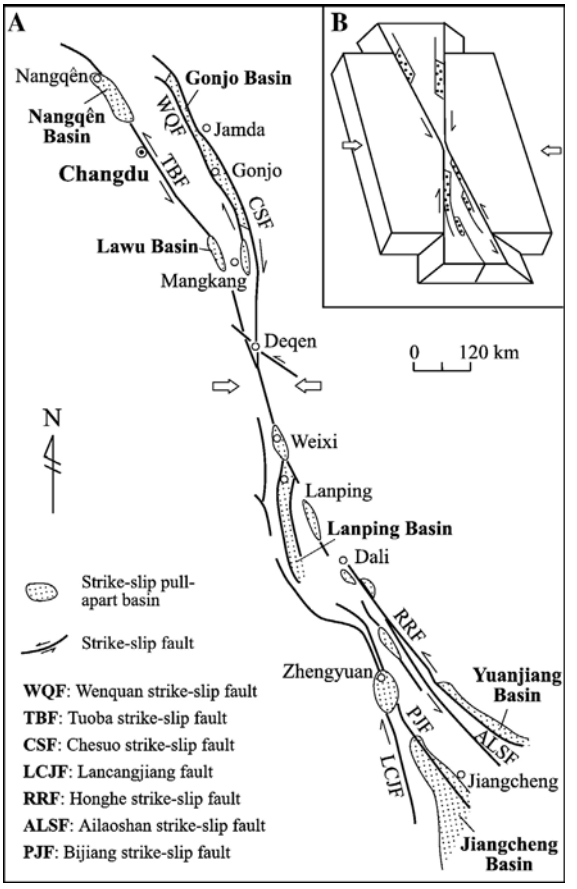

Fig. 18. The strike-slip system and strike-slip pull-apart basins in eastern Tibet (modified from Liu et al., 1993; Hou et al., 2003a). (A) Distribution of the Himalayan strike-slip system and strike-slip pull-apart basin in the Changdu–Simao continental block; (B) mechanical explanation of the strike-slip structure. The northeastward wedging of the Indian continent and subsequent collision with the Yangtze continent during the Late Palaeocene–Eocene caused intense E–W compression and the formation of the conjugate strike-slip fault zones, which produced an 'X'-shaped structural knot with Deqen at the center in the eastern part of the Tibetan Plateau. The transition from single dextral strike-slip fault system to conjugate strike-slip fault zones resulted in stress relaxation, which caused the movement of the blocks bounded by the conjugate fault zones from the Deqen structure knot to the southern and northern ends, and the formation of strike-slip pull-apart basins.

These strike-slip pull-apart basins not only facilitate the ascent and shallow-level emplacement of ore-bearing porphyry magmas (Busell, 1976; Hutton, 1988), as well as constraining the temporal–spatial localization of the Yulong porphyry hydrothermal–magmatic system (Hou et al., 2003a,b), but are also important ore-bearing basins. In these ore-bearing basins, mixing of deep saline (magmatic) fluid with shallow (meteoric) water resulted in the precipitation of large quantities of ore metals (Cu, Pb, Zn, Ag, etc) to

form a number of hydrothermal Ag polymetallic deposits in the epoch.

5.3.2. Large-scale thrust system

Corresponding to the Indian–Asian continent collision, a series of thrust belts were developed in the Sanjiang Tethys, such as the Fenghuoshan–Nangqen thrust belt and the Ailaoshan thrust–shear belt (Figs. 1 and 3; Yin and Harrison, 2000). A 500 km long Ailaoshan–Diancangshan metamorphic belt was developed along the Ailaoshan thrust–shear belt (Tapponnier et al., 1990), and extensive strike-slip movement and thrusting along this shear belt resulted in three thrust faults (e.g., Honghe, Ailaoshan and Jiujia–Mojiang) and several nappes (e.g., Ailaoshan, Yushan, Sanmeng, Lvchun) bounded by these thrust faults (Fig. 3). These nappes, as significant ore-bearing formations, controlled the localization of the Ailaoshan gold ore district. The interlayered *decollement* planes in the nappes commonly host the individual Au deposits and Au orebodies. The intersections of these strike-slip faults with thrust faults might be the main channels for the migration of deep fluids.

6. Summary and conclusions

There are three significant tectonic settings and environments under which large-scale mineralizations occurred in the STMD: 1) an arc-basin system, 2) post-collision crustal extension and 3) large-scale strike-slip fault and thrust systems, corresponding to the three most important metallogenic epochs.

There are three arc-basin systems with different epochs and variable mineralization. Of these, the Yagra-style VHMS deposits occurred in an Early Permian intra-oceanic arc, and were related to the subduction of the Jinshajiang oceanic slab. The Gacun-style VHMS deposits occurred in intra-arc rift basins within the Late Triassic Yidun island-arc related to the Litang slab subduction.

Post-collisional crustal extension occurred in the Late Triassic and was probably caused by lithospheric delamination or slab break-off beneath the Changdu–Simao block. The extensional basins that formed on the Permian continental margin arcs were largely filled by bimodal volcanic successions in the lower part, and gypsum-bearing clastic sequences with associated intermediate–felsic pyroclastic rocks in the upper part. The Luchun-style VHMS Cu deposits were formed in a deep-water marine volcanic environment, whereas the Zhaokalong-style Fe–Ag-polymetallic deposits occurred in a shallow-water volcanic environment in the extensional basins. The rift basins that developed on the Changdu–Simao block were filled by a sequence consisting of siliceous rock, laminar fine-crystalline dolomite and dolomitic limestone, and host most of exhalative-sedimentary Ag-polymetallic deposits.

Large-scale strike-slip fault and thrust systems that occurred in the Sanjiang Tethys were caused by the Indian–Asian continental collision initiated during the Palaeocene. This collision also led to intense shortening and thickening of the crust in the interior Plateau and the formation of the Gangdese-arc granitoid batholiths. The batholith extends eastwards to the Chayu-Tengchong granitoid belt and served as the ore-bearing host for Sn and rare metal ore belts. The large-scale strike-slip faulting systems controlled the temporal–spatial localization of the Yulong porphyry belt and the porphyry hydrothermal–magmatic system. They also resulted in the formation of a series of strike-slip pull-apart basins which constrained long-distance migration and large-scale convection of hydrothermal fluids and which host most of the hydrothermal vein-type and replacement-type Ag–Cu–Pb–Zn deposits. The large-scale thrust system along the Ailaoshan shear zone led to a series of parallel thrust faults and nappes bounded by these faults, which constrain the localization of the Ailaoshan Au belt or ore districts. The interlayered *decollement* zone or thrust fracture-zone controlled individual Au deposits and Au orebodies.

The deposit types in the STMD occur in different metallogenic epochs and display a trend from simple to complex natures corresponding to the tectonic evolution of the Sanjiang Tethys from Early Palaeozoic to the Tertiary. In the Early Palaeozoic metallogenic epoch, mineralization took place only along the boundaries of scattered blocks resulting from the break-off of the continental blocks, and only minor hydrothermal Pb–Zn deposits formed. In the Late Palaeozoic metallogenic epoch, mineralization mainly occurred in arc-basin systems, resulting in a number of VHMS deposits with Cu–Zn, Cu–Pb–Zn and Fe–Cu associations. Entering the Late Triassic, at least three types of ore deposits occurred in the post-collisional crustal extension settings, caused by the lithospheric delamination or slab break-off and the arc-basin system. The VHMS deposits occur in both post-collision extensional basins and intra-arc rift basins, whereas the porphyry Cu deposits and/or skarn-type polymetallic deposits formed in arc volcano-magmatic complexes and the epithermal Ag–Au–Hg deposits in the back-arc felsic volcanic rocks.

In the Himalayan (Tertiary) epoch, metallogensis tended to be more complicated and formed a large number of large or giant deposits of different genetic

types. Four deposit types are significant. The first is the porphyry Cu deposits closely related to the Jinshajiang strike-slip fault system. The second refers to the hydrothermal deposits occurring in strike-slip pull-apart basins on the Changdu–Simao block. The third involves the shear-zone type lode Au deposits related to the large-scale thrust and shear system developed along the Honghe–Ailaoshan fault zone; and the fourth is the granite-related Sn and rare metal deposits in the Chayu–Tengchong granitoid belt. The metallic associations are also more complicated, including (1) enrichment of rare and rare earth elements to form rare metal deposits, (2) extreme enrichment of single elements to form large deposits such as the giant Ailaoshan Au deposit, the large Dongzhiyan Sr deposit, and the giant Yulong Cu deposit, and (3) coexistence of crust-derived elements (e.g., Rb, Pb, Ag and Sr) and mantle-derived elements (e.g., Co, Ni, Au and Cu) in the individual polymetallic deposits.

Acknowledgements

This paper could not have been produced without the excellent support of research geologists and mine geologists working in the Sanjiang region, S.W. China. We are indebted to a large number of researchers who supplied materials on geology and mineral deposits in the Sanjiang region. The authors also would like to thank staff members of the Institute of Mineral Resources, Chinese Academy of Geological Sciences (CAGS), Beijing for constructive discussions and comments. Special thanks are due to reviewers, Professors D. I. Groves and Hansgeorg Forster for their helpful comments in improving this manuscript. This work is supported by the National Basic Research Program (973 Project: No. 2002CB412600).

References

Allegre, C.J., et al., 1984. Structure and evolution of the Himalayan–Tibet orogenic belt. Nature 307, 17–22.

Bird, P., 1979. Continental delamination and the Colorado Plateau. Journal of Geophysical Research 84, 7561–7571.

Busell, M.A., 1976. Fracture control of high-level plutonic contacts in the coastal batholith of Peru. Proceedings of the Geologists' Association 87, 237–246.

Camus, F., Dilles, J.H., 2001. A special issue devoted to porphyry copper deposits of northern Chile—preface. Economic Geology 96, 233–238.

Cathles, L.M., Guber, A.L., Lenagh, T.C., Dudas, F.O., 1983. Kuroko-type massive sulphide deposits of Japan: products of an aborted island-arc rift. Economic Geology Monographs 5, 96–114.

Chen, J.-C., 1987. Chronology and emplacement ages of the granitic rocks in the western Yunnan. Yunnan Geology 6, 101–113 (in Chinese).

Chen, H.-S., 1994. Studies on Isotopic Geochemistry. Zhejiang University Press, Hangzhou. 340 pp. (in Chinese with English abstract).

Chung, S.-L., Lo, C.-H., Lee, T.-Y., Zhang, Y.-Q., Xie, Y.-W., Li, X.-H., Wang, K.-L., Wang, P.-L., 1998. Dischronous uplift of the Tibetan Plateau starting from 40 My ago. Nature 349, 769–773.

Crawford, A.J., Berry, R.F., 1992. Tectonic implications of Late Proterozoic–Early Palaeozoic igneous rock associations in W Tasmania. Tectonophysics 214, 37–56.

Crawford, A.J., Corbett, K.D., Everard, J., 1992. Geochemistry and tectonic setting of a Cambrian VMS-rich volcanic belt: the Mount Read Volcanics, W Tasmania. Economic Geology 87, 597–619.

Carvalho, D., 1991. A case history of the Neves–Corvo massive sulphide deposit, Portugal, and implication for future discoveries. Economic Geology Monographs 8, 314–334.

Davies, J.H., Blanckenburg, F.V., 1995. Slab break-off: a model of lithosphere detachment and its test in the magmatism and deformation of collision orogens. Earth and Planetary Science Letters 129, 85–102.

Dewey, J.F., 1988. Extensional collapse of orogens. Tectonics 7, 1123–1140.

Dong, S.-W., 1999. Tectono-magmatic evolution and metallogeny in the orogens. In: Chen, Y. (Ed.), Theories and Technology of Mineral Resource Exploration and Assessment. Earthquake Press, Beijing, pp. 74–82 (in Chinese).

Du, A.-D., He, H.-L., Yin, W.-N., 1994. The study on the analytical methods of Re–Os age for molybdenites. Acta Geologica Sinica 68, 339–346 (in Chinese with English abstract).

England, P., Molnar, P., 1990. Right-lateral shear and rotating as the explanation for strike-slip faulting in eastern Tibet. Nature 344, 140–142.

Franklin, J.M., Sangster, D.F., Lydon, J.W., 1981. Volcanic-associated massive sulphide deposits. Economic Geology 75th Anniv. Vol., 485–627.

Fukao, Y., Muruyama, S., Inoue, H., 1994. Geologic implication of the whole mantle pave tomography. Journal of the Geological Society of Japan 100, 4–23.

Galley, A.G., Bailes, A.H., Kitzler, G., 1993. Geological setting and hydrothermal evolution of the Chisel Lake and North Chisel Zn–Pb–Cu Ag–Au massive sulphide deposits, Snow Lake, Manitoba. Exploration and Mining Geology 2, 271–295.

Halley, S.W., Roberts, R.H., 1997. Henty: a shallow-water gold-rich volcanogenic massive sulphide deposit in western Tasmania. Economic Geology 92, 438–447.

Hao, Z.-W., Yu, R.-L., Hou, L.-W., 1983. The relationship between Baryankala–Kunlun ocean and Tethyan ocean in southwestern China. Contribution to Geology of the Qinghai–Tibetan Plateau, vol. 11. Geological Publishing House, Beijing (in Chinese).

Harrsion, T.M., Copeland, P., Kidd, W.S.F., Yin, A., 1992. Raising Tibet. Science 255, 1663–1670.

Hou, Z.-Q., 1993. The tectono-magmatic evolution of Yidun island-arc and geodynamic setting of the formation of Kuroko-type massive sulphide deposits in Sanjiang region, southwestern China. Resource Geology 17, 336–350.

Hou, Z.-Q., Mo, X.X., 1993. Geology, geochemistry and genetic aspects of Kuroko-type massive sulphide deposits in Sanjiang, southwestern China. Exploration and Mining Geology 2, 17–29.

Hou, L.-W., Fu, D.-M., Hu, S.-H., Li, K.-Y., Dai, B.-C., Xiao, Y., 1983. Characteristics of magmatism and relation to plate tectonics and mineralization in the western Sichuan and eastern Tibet. Contribution to Geology of the Qinghai–Tibetan Plateau, vol. 13. Geological Publishing House, Beijing (in Chinese).

Hou, Z.-Q., Hou, L.-W., Ye, Q.-T., Liu, F.-L., Tang, G.-G., 1995. Tectono-Magmatic Evolution and Volcanogenic Massive Sulphide Deposits in the Yidun Island-Arc, Sanjiang Region, China. InEarthquake Publishing House, Beijing, pp. 1–218 (in Chinese).

Hou, Z.-Q., Mo, X.-X., Zhu, Q.-W., Shen, S.-W., 1996a. Mantle plume in the Sanjiang Palaeo-Tethyan region, China: evidence from oceanic-island basalts. Acta Geoscientia Sinica 17, 343–361 (in Chinese with English abstract).

Hou, Z.-Q., Mo, X.-X., Zhu, Q.-W., Shen, S.-W., 1996b. Mantle plume in the Sanjiang Palaeo-Tethyan region, China: evidence from mid-ocean ridge basalts. Acta Geoscientia Sinica 17, 362–375 (in Chinese with English abstract).

Hou, Z.-Q., Deng, J., Sun, H.-T., Song, S.-H., 1999. Volcanogenic massive sulphide deposits in China: setting, feature and style. Exploration and Mining Geology 8, 149–175.

Hou, Z.-Q., Zaw, Khin, Qu, X.-M., Ye, Q.-T., Yu, J.-J., Xu, M.-J., Fu, D.-M., Yin, X.-K., 2001a. Origin of the Gacun volcanic-hosted massive sulphide deposit in Sichuan, China: fluid inclusion and oxygen isotope evidence. Economic Geology 96, 1491–1512.

Hou, Z.-Q., Qu, X.-M., Yang, Y.-Q., 2001b. Collision orogeny in the Yidun arc: evidence from granites in the Sanjiang region, China. Acta Geologica Sinica 75, 484–497 (in Chinese with English abstract).

Hou, Z.-Q., Ma, H., Zaw, Khin, Zhang, Y., Wang, M., Wang, Z., Pan, G., Tang, R., 2003a. The Himalayan Yulong porphyry copper belt: product of large-scale strike-slip faulting in eastern Tibet. Economic Geology 98, 125–145.

Hou, Z.-Q., Wang, L., Zaw, Khin, Mo, X., Wang, M., Li, D., Pan, G., 2003b. Post-collisional crustal extension setting and VHMS mineralization in the Jinshajiang orogenic belt, southwestern China. Ore Geology Reviews 22, 177–199.

Hou, Z.-Q., Du, A.-D., Wang, S.-X., Qu, X.-M., Sun, W.-D., 2003c. Re-Os dating of sulfides from the volcanogenic massive sulfide deposit at Gacun, southwestern China. Resource Geology 53, 305–310.

Hou, Q.-Z., Zeng, P.-S., Gao, Y.-F., 2006. The Himalayan Cu-Mo-Au mineralization in the eastern Indo-Asian collision zone: constraints from Re-Os dating of molybdenite. Minerlium Deposita 41, 33–45.

Hu, S.-H., Luo, Z.-W., Zeng, Y.-J., Ren, C.-S., 1992. Volcano-Sedimentary Sequences in the Yidun Island-Arc, Sichuan Province. Geological Publishing House, Beijing. 127 pp. (in Chinese with English abstract).

Hu, Y.-Z., Tang, S.-C., Wang, H.-P., Yang, Y.-Q., Deng, J., 1995. Geology of the Ailaoshan Gold Deposits. Geological Publishing House, Beijing. 278 pp. (in Chinese with English abstract).

Hu, R.-Z., Zhong, H., Ye, Z.-J., Bi, X.-W., Turne, R.G., Burnard, P.G., 1998. Helium–argon isotopic geochemistry of the superlarge Jinding deposit. Science in China 28, 208–213.

Huang, J.-Q., Chen, B.-W., 1987. The Evolution of the Tethys in China and Surrounding Area. Geological Publishing House, Beijing. 256 pp. (in Chinese with English abstract).

Huang, Z.-L., Wang, L.-K., 1996. Geochemistry of lamprophyres in the Laowangzhai gold mine:. Yunnan Geochimica 25, 255–263 (in Chinese with English abstract).

Huang, Z.-L., Wang, L.-K., Zhu, C.-M., 1997. Petrological study of lamprophyres in the Laowangzhai gold mine. Yunnan Geological Sciences 32, 74–87 (in Chinese with English abstract).

Hutton, D.H.W., 1988. Granite emplacement mechanism and tectonic controls: inference from deformation studies. Transactions of the Royal Society Edinburgh. Earth Sciences 79, 245–255.

Iizasa, K., Fiske, R.S., Ishizaka, O., Yuasa, M., Hashimoto, J., Ishibashi, J., Naka, J., Horii, Y., Fujiwara, Y., Imai, A., Koyama, S., 1999. A Kuroko-type polymetallic sulphide deposit in a submarine silicic caldera. Science 283, 975–977.

Jue, M.-Y., 1998. Copper Deposits in the Lanping–Simao Basin. Geological Publishing House, Beijing. 189 pp. (in Chinese with English abstract).

Kay, S.M., 1994. Young mafic back arc volcanic rocks as indicators of continental lithospheric delamination beneath the Argentine Pona Plateau, central Andes. Journal of Geophysical Research 99, 24323–24339.

Kay, R.W., Kay, S.M., 1994. Delamination and delamination magmatism. Tectonophysics 219, 177–189.

Large, R.R., 1992. Australian volcanic-hosted massive sulphide deposits: features, styles and genetic models. Economic Geology 87, 469–470.

Lehman, B., 1990. The Bolivian tin province and regional tin distribution in the central Andes: a reassessment. Economic Geology 85, 1244–1258.

Letouzey, J., Kimura, M., 1986. The Okinawa Trough: genesis of a back-arc basin developing along a continental margin. Tectonophysics 125, 209–230.

Li, N., Kyle, J.R., 1997. Geologic controls of sandstone-hosted Zn–Pb–(Sr) mineralization, Jinding deposit, Yunnan province, China—a new environment for sediment-hosted Zn–Pb deposits. Proceedings, 30th International Geological Congress, vol. 9, pp. 67–82.

Li, X.-Z., Liu, Z.-Q., 1991. The division and evolution of the tectonic units in the Sanjiang region, southwestern China. Bulletin of Chengdu Institute of Geology and Mineral Resources 13, 1–10 (in Chinese).

Li, Y.-Q., Rui, Z.-Y., Cheng, L.-X., 1981. Fluid inclusions and mineralization of the Yulong porphyry copper (Mo) deposit. Acta Geosinitia Sinica 55, 18–23 (in Chinese with English abstract).

Li, X.-Z., Liu, W.-J., Wang, Y.-Z., Zhu, Q.-W., 1999. Tectonic Evolution of the Tethys and Mineralization in the Sanjiang Region, S. W. China. Geological Publishing House, Beijing. 258 pp. (in Chinese with English abstract).

Li, D.-M., Chen, K.-X., Wang, L.-Q., Xu, T.-R., Diao, Z.-Z., 2000. Tectonic evolution and Cu–Au metallogeny in the Jinshajiang orogenic belt. Open file in the Chengdu Institute of Geology and Mineral Resources. 253 pp. (in Chinese).

Liu, B.-J., 1993. Crustal Evolution and Metallogeny in the Palaeo-Continent, Southern China. Science Press, Beijing. 320 pp. (in Chinese with English abstract).

Liu, Z.-Q., Li, X.-Z., Ye, Q.-T., Luo, J.-N., Shen, G.-F., 1993. Division of Tectono-Magmatic Zones and the Distribution of Deposits in the Sanjiang Area. Geological Publishing House, Beijing. 246 pp. (in Chinese with English abstract).

Lu, B.-X., Wang, Z., 1993. Granitoid and Related Mineralization in the Sanjiang Region. Geological Publishing House, Beijing. 258 pp. (in Chinese with English abstract).

Luo, J.-L., Yang, Y.-H., Zhao, Z.-W., 1994. Tectonic Evolution of the Tethys and Metallogeny in the Western Yunnan. Geological Publishing House, Beijing. 235 pp. (in Chinese with English abstract).

Lydon, J.W., 1988. Ore deposit models #14 volcanogenic massive sulphide deposits. Part 2: genetic models. Geoscience Canada 15, 43–65.

Ma, H.-W., 1990. Granitic Rocks and Mineralization in the Yulong Porphyry Copper Belt, Eastern Tibet. Press of China University

of Geosciences, Beijing. 157 pp. (in Chinese with English abstract).

Mo, X.-X., Lu, F.-X., Shen, S.-Y., Zhu, Q.-W., Hou, Z.-Q., 1993. Volcanism and Metallogeny in the Sanjiang Tethys. Geological Publishing House, Beijing. 250 pp. (in Chinese with English abstract).

Pan, G.-T., Chen, Z.-L., Li, X.-Z., 1997. Tectonic Evolution of the East Tethys Geology. Geological Publishing House, Beijing. 257 pp. (in Chinese with English abstract).

Peltzer, G., Tapponnier, P., 1988. Formation and evolution of strike-slip faults, rifts and basins during the India–Asia collision: an experimental approach. Journal of Geophysical Research 93, 15085–15117.

Powell, C.M.A., 1986. Continental underplating model for the rise of the Tibetan plateau. Earth and Planetary Science Letters 81, 79–94.

Qu, X.-M., Hou, Z.-Q., Zhou, S.-G., 2001. Geology and mineralization characteristics of the Lianlong skarn-type polymetallic deposit in Western Sichuan. Acta Geoscientica Sinica 22, 29–34 (in Chinese with English abstract).

Ren, J.-S. (Ed.), 1987. Regional Tectonic and Evolution in China. InGeological Publishing House, Beijing. 231 pp. (in Chinese).

Richard, D., 1999. European Phanerozoic metallogenesis. Mineralium Deposita 34, 417–421.

Rona, P.A., 1984. Hydrothermal mineralization at seafloor spreading centers. Earth-Science Reviews 20, 1–104.

Rona, P.A., Scott, S.D., 1993. A special issue on seafloor hydrothermal mineralization: new perspectives—preface. Economic Geology 88, 1933–1976.

Rui, Z.-Y., Huang, Z.-K., Qi, G.-M., Xu, J., Zhang, H.-T., 1984. Porphyry Cu (–Mo) Deposits in China. Geological Publishing House, Beijing. 350 pp. (in Chinese).

Sacks, P.E., Secor Jr., D.T., 1990. Delamination in collisional orogens. Geology 18, 999–1002.

Sangster, D.F., 1972. Precambrian volcanogenic massive sulphide deposits in Canada. A review. Canada Geol. Survey Paper, vol. 72-22. 44 pp.

Sengor, A.M.C., 1989. The Tethyside orogenic system: an introduction. In: Sengor, A.M.C. (Ed.), Tectonic Evolution of the Tethyan Region. Academic Publishers, pp. 1–22.

Stuart, F.M., Burnard, P.G., Talor, R.P., 1995. Resolving mantle and crustal contributions to hydrothermal fluids: He–Ar isotopes in fluid inclusions from Dae Hwa W.—Mo mineralization, South Korea. Geochimica et Cosmochimica Acta 59, 4663–4673.

Tang, R.-L., Luo, H.-S., 1995. The Geology of Yulong Porphyry Copper (Molybdenum) Ore Belt, Xizang (Tibet). Geological Publishing House, Beijing. 320 pp. (in Chinese with English abstract).

Tapponnier, P., Molnar, P., 1976. Slip-line field theory and large-scale continental tectonics. Nature 264, 319–324.

Tapponnier, P., Lacassin, R., Leloup, P.H., Scharer, U., Zhong, D.-L., Haiwei, W., Liu, X.-H., Ji, S.-C., Zhang, L.-S., Zhong, J.-Y., 1990. The Ailao Shan/Red River metamorphic belt: Tertiary left-lateral shear between Indochina and South China. Nature 343, 431–437.

Wang, J.-H., Yan, W., 1998. Hydrothermal Sedimentary Processes on the Continent: an Example From Yunnan Area. Geological Publishing House, Beijing. 189 pp. (in Chinese).

Wang, L.-Q., Pan, G.-T., Li, D.-M., 1999a. Spatial-temporal architecture and tectonic evolution of the Jinshajiang arc-basin system. Acta Geologica Sinica 73, 206–218 (in Chinese with English abstract).

Wang, X.-F., Metcalfe, L., Jian, P., 1999b. Division of tectono-strata and geological date for the Jinshajiang suture zone. Science in China 29, 290–296 (in Chinese).

Wang, C.-S., Gu, X.-X., Chen, J.-P., 2000a. Evolution of the Lanping basin and metallogenic environments. Open File of the Chengdu Technological Institute. . 261 pp. (in Chinese).

Wang, M.-J., Peng, Y.-M., Wang, G.-M., Shentu, B.-Y., Yao, P., Chen, M., 2000b. Evolution and ore-forming conditions of the Changdu basin. Open File, Chengdu Institute of Geology and Mineral Resources. 268 pp. (in Chinese).

Wang, L.-Q., Hou, Z.-Q., Mo, X.-X., Wang, M.-J., Xu, Q., 2002. Post-collisional extension: a new environment for VHMS deposits in the Jinshajiang orogenic belt. Scientia Geologica Sinica 76, 541–556 (in Chinese with English abstract).

Xiao, X.-C., 1983. Yalu Zongbu suture zone and its tectonic evolution in the surrounding area. Acta Geologica Sinica 57, 205–212 (in Chinese with English abstract).

Xiao, R.-G., Chen, H.-Q., 1991. Characteristics and hydrothermal boiling origin for copper mineralization in the Lanping Mesozoic–Cenozoic basin, Yunnan. Bulletin of Mineralogy, Petrology and Geochemistry 2, 35–37 (in Chinese).

Xu, M.-J., Fu, D.-M., Yin, Y.-M., Yin, X.-K., Xian, X.-M., Xiao, Y., 1993. Gacun Ag-Rich Polymetallic Deposit in Sichuan Province, China. Publishing House of Chengdu University of Science and Technology, Sichuan. 164 pp. (in Chinese with English abstract).

Xue, C.-J., Wang, D.-H., Chen, Y.-C., Yang, J.-M., Yang, W.-G., 2000. Helium, argon, and xenon isotopic compositions of ore-forming fluids in Jinding–Baiyangping polymetallic deposits, Yunnan, southwestern China. Acta Geologica Sinica 74, 512–518.

Yan, K.-M., Geng, S.-F., 1993. New progress and new understanding on the Qinling–Bashan and surrounding area. Regional Geology of China, vol. 4. Geological Publishing House, Beijing. (in Chinese).

Yang, K., Mo, X., 1993. Volcanogenic massive sulfide deposits in Southwestern China. Resource Geology 17, 263–276.

Yang, K.-H., Hou, Z.-Q., Mo, X.-X., 1992. Characteristics and genetic types of volcanogenic massive sulphide deposits in Sanjiang region. Mineral Deposits 11, 35–44 (in Chinese with English abstract).

Yang, Y.-Q., Wang, W.-Y., Yu, J., 2000. Geology and geochemistry studies on the Dapingzhang VMS deposit in western Yunnan, southwestern China. Open File, Institute of Mineral Resource. 120 pp. (in Chinese).

Ye, Q.-T., Shi, G.-H., Ye, J.-H., Yang, C.-Q., 1992. Geological Characteristics and Mineralogenic Series of the Lead–Zinc Deposits in Sanjiang Region. Scientific and Technical Publishing House of Beijing. 175 pp. (in Chinese with English abstract).

Ye, Q.-T., Hu, Y.-Z., Yang, Y.-Q., 1993. Regional Geochemical Background and Gold, Silver, Lead, Zinc Mineralization in the Sanjiang Region, S.W. China. Geological Publishing House, Beijing. 253 pp. (in Chinese with English abstract).

Yin, Y., Harrison, T.M., 2000. Geologic evolution of the Himalayan–Tibetan orogen. Annual Review of Earth and Planetary Sciences 28, 211–280.

Zhan, M.-G., Lu, Y.-F., Chen, S.-F., 1998. The Yargla Copper Deposit in Deqen, Western Yunnan. Publishing House of the China University of Geosciences, Wuhan. 187 pp. (in Chinese with English abstract).

Zhang, G.-W., 1988. Origin and Evolution of the Qinling Orogen. Northwestern University Press, Xi'an. 246 pp. (in Chinese).

Zhang, Y.-Q., Xie, Y.-W., 1997. Chronology and Nd–Sr isotopes of the Ailaoshan–Jinshajiang alkali-rich intrusions. Sciences in China 27, 289–293 (in Chinese).

Zhang, N.-D., Cao, Y.-W., Liao, Y.-A., Zhao, Y., Zhang, H.-J., Hu, D.-O., Zhang, R., Wang, L.-B., 1998a. Geology and Metallogeny in the Garze–Litang Rift Zone. Geological Publishing House, Beijing. 119 pp. (in Chinese).

Zhang, Y.-Q., Xie, Y.-W., Liang, H.-Y., Qiu, H.-N., Li, X.-H., Zhong, S.-L., 1998b. Petrogenesis series and the ore-bearing porphyries of the Yulong copper ore belt in eastern Tibet. Geochimica 27, 236–243 (in Chinese with English abstract).

Zhang, Y.-Q., Xie, Y.-W., Qiu, H.-N., Li, X.-H., Zhong, S.-L., 1998c. Shoshonitic series: Sr, Nd, and Pb isotopic compositions of ore-bearing porphyry for Yulong copper ore belt in the eastern Xizang (Tibet). Scientia Geologica Sinica 33, 359–366 (in Chinese with English abstract).

Zhang, Y.-Q., Xie, Y.-W., Li, X.-H., 2000. Isotope features of magmatic rocks of the shoshonitic series in the eastern Qinghai–Tibet Plateau: origin of the rocks and their tectonic significance. Science in China 30, 493–498 (in Chinese).

Zhong, D.-L., Ding, L., Liu, F.-T., Liu, J.-H., Zhang, J.-J., Ji, J.-Q., Chen, H., 2001. Poly-layered architecture of lithosphere in orogen and its constraint on Cenozoic magmatism—example from Sanjiang and surrounding area. Science in China 30, 1–8 (in Chinese).